UNIVERSITÀ
DI PAVIA

Dipartimento di Biologia e Biotecnologie
"Lazzaro Spallanzani"

Laurea Magistralis in Molecular Biology and Genetics

Investigation into the molecular mechanism of temperature-dependent γ-PGA production in *Bacillus subtilis*

Indagine sul meccanismo molecolare della produzione temperatura-dipendente di γ-PGA in *Bacillus subtilis*

Supervisor:

Prof. Cinzia Calvio

Experimental thesis by

Abdullah Seyhan

Academic Year 2025/2026

Abstract

Poly-γ-glutamic acid (γ-PGA) is an extracellular polymer produced by *Bacillus subtilis* with diverse biological and biotechnological applications. The γ-PGA biosynthetic operon, *pgs*, is activated by phosphorylated DegU (DegU-P) and SwrA. The DegS-DegU two-component system is a well-characterized regulatory pathway that controls a wide range of physiological processes occurring during the stationary phase of growth in *B. subtilis*. Conversely, much less is known about the small regulatory protein SwrA, despite its established roles in bacterial motility and γ-PGA production, both mediated by its interaction with DegU-P.

γ-PGA production is strongly influenced by environmental conditions, including temperature, but the regulatory mechanisms underlying its temperature dependence remain obscure. This study investigates the molecular mechanisms underlying temperature-dependence of γ-PGA biosynthesis in *B. subtilis*, addressing the contributions of SwrA and DegU-P.

It was verified that *pgsB* expression, which reflects the activation of the γ-PGA biosynthetic pathway, was substantially reduced at 24 °C compared with 37 °C. Analysis of *swrA* mRNA secondary structure predictions identified a potential hairpin structure that could sequester the ribosome-binding site at lower temperatures, functioning as a potential RNA thermometer. To test this hypothesis, a targeted mutation was introduced to disrupt the predicted structure and its potential role in temperature-dependent *swrA* expression was investigated.

It was shown that the mutation did not restore γ-PGA production at 24 °C. Furthermore, the wild-type swrA allele showed higher expression than the mutant swrA allele at both 24 °C and 37 °C. Consistent with this observation, *swrA* overexpression from an inducible promoter did not restore γ-PGA production at 24 °C.

In addition, *aprE* expression, known to be induced by DegU-P alone and on which SwrA has a negative impact, was investigated as a readout of DegU-P activity. In a Δ*swrA* background, *aprE* expression was strongly reduced at 24 °C compared with 37 °C. Together, these findings indicate that the temperature dependence of γ-PGA production is primarily associated with reduced DegU-P activity at 24 °C rather than with temperature-dependent *swrA* expression. The mechanism that controls the temperature-dependence of DegU-P activity remains to be investigated.

Abstract

L'acido poli-γ-glutammico (γ-PGA) è un polimero extracellulare prodotto da *Bacillus subtilis* con diverse applicazioni biologiche e biotecnologiche. L'operone biosintetico del γ-PGA, *pgs*, è attivato dalla forma fosforilata di DegU (DegU-P) e da SwrA. Il sistema a due componenti DegS-DegU è un sistema di regolazione ben caratterizzato che controlla un'ampia gamma di processi fisiologici che avvengono durante la fase stazionaria della crescita in *B. subtilis*. Al contrario, si sa molto meno sulla proteina regolatoria SwrA, nonostante il suo ruolo consolidato nella motilità batterica e nella produzione di γ-PGA, entrambi mediati dalla sua interazione con DegU-P.

La produzione di γ-PGA è influenzata dalle condizioni ambientali, tra cui la temperatura, ma i meccanismi di regolazione alla base della sua dipendenza dalla temperatura rimangono oscuri. Questo studio analizza i meccanismi molecolari alla base della dipendenza dalla temperatura della biosintesi del γ-PGA in *B. subtilis*, esaminando il contributo di SwrA e DegU-P.

È stato verificato che l'espressione di *pgsB*, che riflette l'attivazione della via biosintetica del γ-PGA, risulta sostanzialmente ridotta a 24 °C rispetto a 37 °C. L'analisi delle predizioni della struttura secondaria dell'mRNA di *swrA* ha identificato una potenziale struttura a forcina (hairpin) che potrebbe sequestrare il sito di legame del ribosoma a bassa temperatura, fungendo da potenziale termometro a RNA. Per verificare questa ipotesi, è stata introdotta una mutazione mirata a destabilizzare la struttura predetta, ed è stato studiato il suo potenziale ruolo nell'espressione di *swrA* dipendente dalla temperatura.

I risultati hanno mostrato che la mutazione non ha ripristinato la produzione di γ-PGA a 24 °C. Inoltre, l'allele *swrA* wild-type ha mostrato un'espressione maggiore rispetto all'allele *swrA* mutante sia a 24 °C sia a 37 °C. In linea con questa osservazione, la sovraespressione di *swrA* da un promotore inducibile non ha ripristinato la produzione di γ-PGA a 24 °C.

Inoltre, l'espressione di *aprE*, nota per essere indotta solo da DegU-P e sulla quale SwrA ha un impatto negativo, è stata studiata come indicatore dell'attività di DegU-P. In un background Δ*swrA*, l'espressione di *aprE* è risultata fortemente ridotta a 24 °C rispetto a 37 °C. Insieme, questi risultati indicano che la dipendenza dalla temperatura della produzione di γ-PGA è associata principalmente a una ridotta attività di DegU-P a 24 °C, piuttosto che a un'espressione di *swrA* dipendente dalla temperatura. Il meccanismo che controlla la dipendenza dalla temperatura dell'attività di DegU-P resta ancora da chiarire.

Table of Contents

1.0 Introduction

1.1 *Bacillus subtilis*

Bacillus subtilis is a Gram-positive, rod-shaped bacterium that was first described by Ferdinand Cohn in 1872 and has been extensively studied for more than a century. It is widely distributed across diverse environments, including soil, plants, and the gastrointestinal tracts of animals [1].

B. subtilis has been used as a model organism because of its safety, rapid growth, ease of cultivation, and ability to undergo natural genetic transformation. Its capacity to form endospores and transition between distinct physiological states has also made it a valuable system for investigating fundamental biological processes beyond sporulation, including cellular differentiation, biofilm formation, and competence [2].

The genetic accessibility of *B. subtilis* makes it particularly well suited for genetic studies. The completion of its genome sequence in 1997 provided a comprehensive foundation for investigating its genetic composition and regulatory mechanisms. Its genome is also among the best-annotated bacterial genomes, with successive updates providing increasingly detailed information about its genetic content [1,2]. The availability of versatile genetic tools has further facilitated the study and manipulation of *B. subtilis*, enabling detailed investigations of its biology and regulatory mechanisms as well as its use in various biotechnological applications.

Moreover, *B. subtilis* exhibits remarkable physiological versatility, with genetically identical cells capable of adopting distinct cellular states in response to environmental and physiological conditions [3]. Depending on the conditions encountered, subpopulations can differentiate into motile cells, competent cells, extracellular matrix-producing cells, or cells that secrete degradative enzymes and toxins. Under conditions that are unfavorable for continued growth, a subset of cells can enter sporulation and develop into highly resistant endospores. The ability to generate distinct cell types allows *B. subtilis* populations to coordinate different physiological activities and adapt to changing environmental conditions [3,4].

Among the different physiological states adopted by *B. subtilis*, biofilm formation represents an important strategy for survival and persistence under changing environmental conditions. This ability to establish stable microbial communities is particularly relevant to agricultural applications. Persistence and colonization of plant roots are important for the plant growth-promoting and biocontrol activities of *B. subtilis* [5]. The same properties have also attracted

interest in environmental and industrial applications, in which *B. subtilis* biofilms can be exploited for processes such as wastewater treatment and bioremediation [6].

Beyond its ecological roles, *B. subtilis* has also gained considerable importance in biotechnology as a versatile microbial cell factory. Its efficient secretion systems enable the production and release of a wide range of extracellular enzymes and recombinant proteins directly into the culture medium, simplifying downstream processing [7]. In addition, its extensive genetic engineering toolbox enables the modification of metabolic pathways and regulatory elements to enhance the production of diverse compounds, including vitamins, metabolites, antimicrobial peptides, and biopolymers [8]. These properties, together with its established use in large-scale fermentation, have made *B. subtilis* an important platform for the industrial production of enzymes and other valuable biological products [7,8].

1.2 Two-Component Systems

Bacteria constantly encounter changes in their surrounding environment and must adjust their physiology accordingly to maintain growth and survival. Two-component systems (TCSs) are widely conserved signaling mechanisms that allow bacteria to sense environmental and intracellular cues and coordinate appropriate cellular responses. They regulate various aspects of bacterial cell physiology, including resistance to physical and chemical stresses, cell division, biofilm formation, quorum sensing, and sporulation [9]. In pathogenic bacteria, TCSs can also contribute to virulence by regulating cellular responses to conditions encountered within the host [10].

The archetypal TCS consists of two components: a sensor histidine kinase (HK) and a response regulator (RR). The HK generally contains an N-terminal sensor region that detects a specific environmental or intracellular signal and a C-terminal kinase domain responsible for phosphorylation. Upon sensing the appropriate signal, the HK undergoes autophosphorylation at a conserved histidine residue using ATP. The phosphoryl group is subsequently transferred from the HK to a conserved aspartate residue within the receiver domain of the RR. Phosphorylation induces a conformational change in the RR, promoting its active state and enabling it to regulate downstream cellular processes. In many TCSs, the RR contains a DNA-binding domain that directly controls the transcription of target genes, thereby linking environmental sensing to changes in gene expression [11].

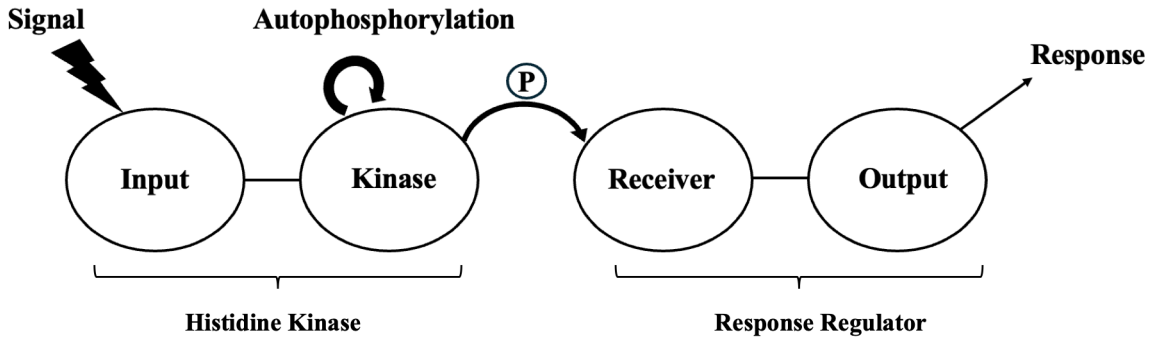

Figure 1.1. General mechanism of a bacterial two-component signal transduction system.

In some signaling pathways, phosphorylation is transmitted through additional protein intermediates rather than directly from the HK to the RR. These pathways, known as phosphorelays, involve a series of sequential phosphotransfer reactions in which the phosphoryl group is passed between multiple components before reaching the final response regulator. This additional level of organization provides opportunities for signal integration and regulation, allowing bacteria to precisely control complex physiological processes [12]. In *B. subtilis*, the Spo0A phosphorelay is a well-characterized example in which phosphoryl groups are transferred from several histidine kinases through intermediate relay proteins to the response regulator Spo0A (Figure 1.2). Accumulation of phosphorylated Spo0A (Spo0A~P) above a critical level initiates sevral transcriptional programs typical of stationary phase, ultimately leading to sporulation [13].

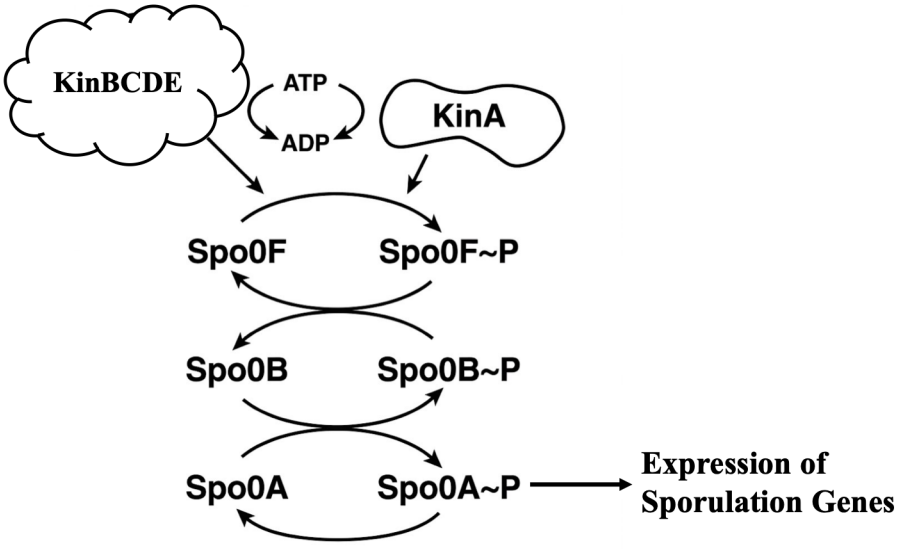

Figure 1.2. Schematic representation of the Spo0A phosphorelay system in *Bacillus subtilis*, adapted from [13].

B. subtilis possesses more than 30 TCSs, making them a major component of its regulatory network. These systems differ in the signals they detect and the cellular responses they control, allowing *B. subtilis* to regulate distinct physiological processes through dedicated signaling pathways [14]. Several of these systems have well-characterized roles in processes such as competence, cell wall homeostasis, and sporulation.

One well-characterized example is the ComP-ComA two-component system, which regulates the development of genetic competence in *B. subtilis*. When the population reaches a suitable physiological and environmental state, extracellular ComX pheromone is detected by the sensor histidine kinase ComP, leading to its autophosphorylation and subsequent transfer of the phosphoryl group to the response regulator ComA. Phosphorylated ComA activates the expression of genes required for the development of competence, enabling cells to take up extracellular DNA and incorporate new genetic information into their genome [15].

Another important example is the WalK-WalR two-component system, which plays a central role in maintaining cell wall homeostasis in *B. subtilis*. Although the precise signal sensed by WalK remains incompletely understood, its activity is closely linked to cell wall growth and remodeling. The sensor histidine kinase WalK phosphorylates the response regulator WalR, which regulates the expression of genes involved in cell wall metabolism and remodeling. Proper regulation of WalK-WalR signaling is therefore essential for maintaining cell envelope integrity and bacterial viability during growth and changing environmental conditions [16].

Finally, the DegS-DegU system is one of the best-characterized TCSs in *B. subtilis* and regulates several important physiological processes, including biofilm formation, motility, extracellular protease production, and γ-PGA synthesis [17,18]. The role of this system in regulating γ-PGA production is particularly relevant to the work presented in this thesis and will be discussed in greater detail in the following section.

1.3 DegS-DegU Two Component System

The DegS-DegU two-component system is a major regulatory pathway in *B. subtilis* that coordinates the expression of more than hundred genes involved in adaptation to environmental and nutritional changes. It was originally identified through its role in regulating the production of degradative enzymes, which gave the system its name, but subsequent studies have established

DegS-DegU as a broader regulator of processes including motility, competence, biofilm formation, and γ-PGA production [17-20].

DegS functions as the sensor histidine kinase, while DegU serves as the response regulator. Unlike many bacterial histidine kinases, DegS lacks transmembrane domains and functions as a cytosolic kinase. Most two-component histidine kinases are transmembrane proteins activated by extracellular signals sensed through an N-terminal domain protruding from the cell surface. Although the precise mechanism of DegS activation remains incompletely understood, several lines of evidence suggest that the flagellum is involved in this sensing process. Initial studies showed that genetic or mechanical perturbation of flagellar rotation increased *degU* phosphorylation and DegU-P-dependent processes, including *aprE* expression and γ-PGA production [21]. These effects were dependent on the presence of DegS, as they were not observed in *degS* deletion strains. These observations initially led to the hypothesis that inhibition of flagellar rotation serves as the signal activating DegS–DegU signalling. However, subsequent experiments demonstrated that cells with non-functional or structurally altered flagella could retain rotating flagellar motors while still displaying increased DegU-P activity [22]. These findings suggested that flagellar rotation itself is unlikely to be the primary signal. Instead, they support a model in which the mechanical or viscous load experienced by the flagellar apparatus is sensed and influences DegS–DegU signalling. Nevertheless, the existing evidence does not provide a complete explanation of how flagellar sensing leads to DegS activation, and the mechanism of DegS activation remains unclear and requires further investigation.

Upon activation, DegS autophosphorylates at a conserved histidine residue and subsequently transfers the phosphoryl group to a conserved aspartate residue of DegU, generating phosphorylated DegU (DegU-P). DegU-P then regulates the expression of target genes involved in several physiological processes. The phosphorylation of DegU is reversible, as DegS also possesses phosphatase activity that promotes the dephosphorylation of DegU-P, allowing the system to ignore spurious signals and adjust DegU activity to real cellular needs [18,19].

The *degS* and *degU* genes are organized in the *degSU* operon, with *degS* located upstream of *degU*. The *degSU* operon, previously named *sacU*, contains three promoters that allow the expression of *degS* and *degU* to be regulated under different physiological conditions. The first promoter is located upstream of *degS* and drives the expression of both genes, while a second promoter located within *degS* increases *degU* expression under nitrogen-limiting conditions. A third promoter,

located in the *degS-degU* intergenic region, is activated by DegU-P and therefore provides positive autoregulation [18-20].

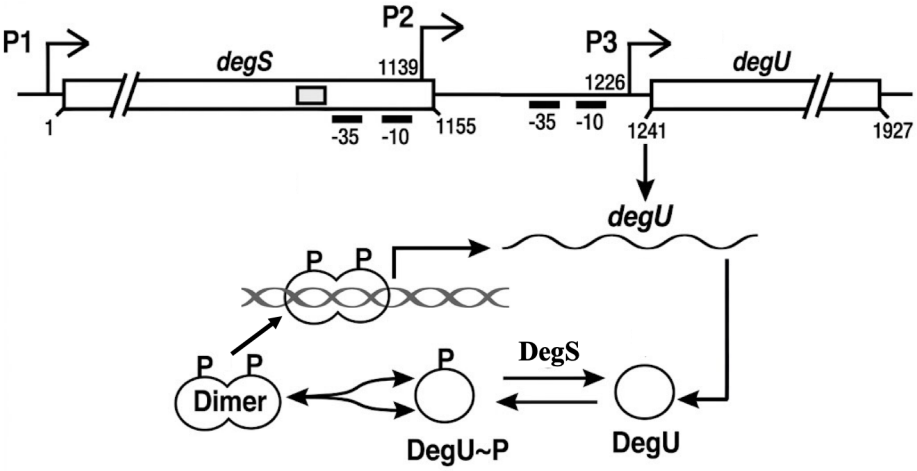

Figure 1.3. Genetic organization and autoregulation of the *degSU* operon, adapted from [18,19].

DegU phosphorylation is further regulated by DegQ, which provides a link between quorum sensing and the DegS–DegU signaling pathway. Under conditions of high cell density, activation of the ComP–ComA quorum-sensing system leads to phosphorylation of ComA. ComA-P then activates transcription of *degQ*, increasing the cellular level of DegQ. DegQ promotes the transfer of the phosphoryl group from DegS to DegU, thereby increasing the level of DegU-P. Through this mechanism, changes in cell density can be transmitted to the DegS–DegU system and ultimately influence the expression of DegU-dependent genes [17,20].

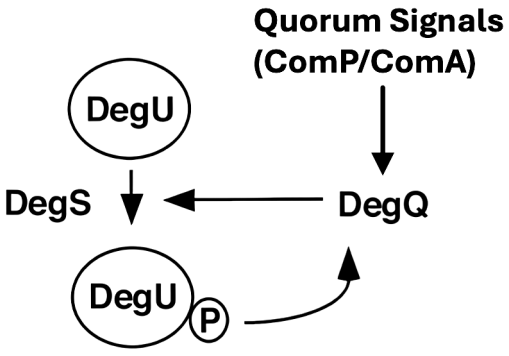

Figure 1.4. Regulation of the DegS–DegU two-component system by DegQ. Quorum signals act through the ComP/ComA system to induce expression of DegQ, which enhances phosphotransfer from DegS to DegU, increasing cellular levels of DegU-P.

The response to DegU-P is not uniform across its target genes. Different promoters have different affinities for DegU-P, allowing changes in DegU phosphorylation to produce distinct transcriptional responses. For example, the *fla/che* promoter, encoding genes for flagellar synthesis, has a higher affinity for DegU-P than the *sacB* promoter, producing levansucrase, suggesting that genes controlled by high-affinity promoters can respond at lower levels of DegU-P, whereas genes requiring higher DegU-P levels are activated later. DegU can also regulate gene expression in its unphosphorylated state, although its regulatory activity differs from that of DegU-P [15]. Unphosphorylated DegU has been shown to promote the expression of *comK* involved in genetic competence [20]. This provides a mechanism by which *B. subtilis* can coordinate different physiological responses through changes in the level of a single response regulator.

Table 1.1. Relationship between DegU phosphorylation state and the regulation of distinct physiological processes in *Bacillus subtilis*.

DegU state	Major regulatory outcome	Representative targets
DegU	Genetic competence	*comK*
Low DegU-P	Motility	*fla/che*
High DegU-P	Exoprotease production, biofilm formation, γ-PGA production	*aprE*, *nprE*, *sacB*, *bslA*, *pgsBCA*

Several mutations in the *degSU* system produce the pleiotropic Hy phenotype (hyperproduction of degradative enzymes), characterized by increased production of extracellular enzymes [23]. These mutations alter DegS-DegU signaling and increase the cellular level or stability of DegU-P. Among the Hy mutants, *degU32(Hy)* and *degS200(Hy)* both result in increased levels of DegU-P but affect the signaling pathway differently. The *degU32(Hy)* allele carries an H12L substitution in DegU that increases the stability of DegU-P but also impairs its interaction with SwrA [24]. Consequently, studies using *degU32(Hy)* may not fully reflect DegU-P regulation in the presence of functional SwrA [25]. In contrast, the *degS200(Hy)* mutation affects the sensor kinase DegS by reducing its phosphatase activity, resulting in the accumulation of phosphorylated wild-type DegU while preserving its ability to interact with SwrA. This distinction is particularly important because SwrA can modulate the activity of DegU-P at target promoters, including those involved in

motility and other DegU-regulated processes [24-25]. Therefore, *degS200(Hy)* provides a more appropriate genetic background for studying DegU-P dependent regulation.

1.4 SwrA

SwrA is a small regulatory protein of 117 amino acids that plays an important role in bacterial swarming motility. It is shown that SwrA is required for the swarming motility of *Bacillus subtilis*, while its absence slightly affects swimming motility [26]. Laboratory strains of *B. subtilis* frequently carry a frameshift mutation in *swrA* caused by an additional adenine within an eight-adenine homopolymeric tract. This mutation disrupts SwrA production and results in a non-swarming phenotype, whereas restoration of the functional *swrA* allele restores swarming motility [27].

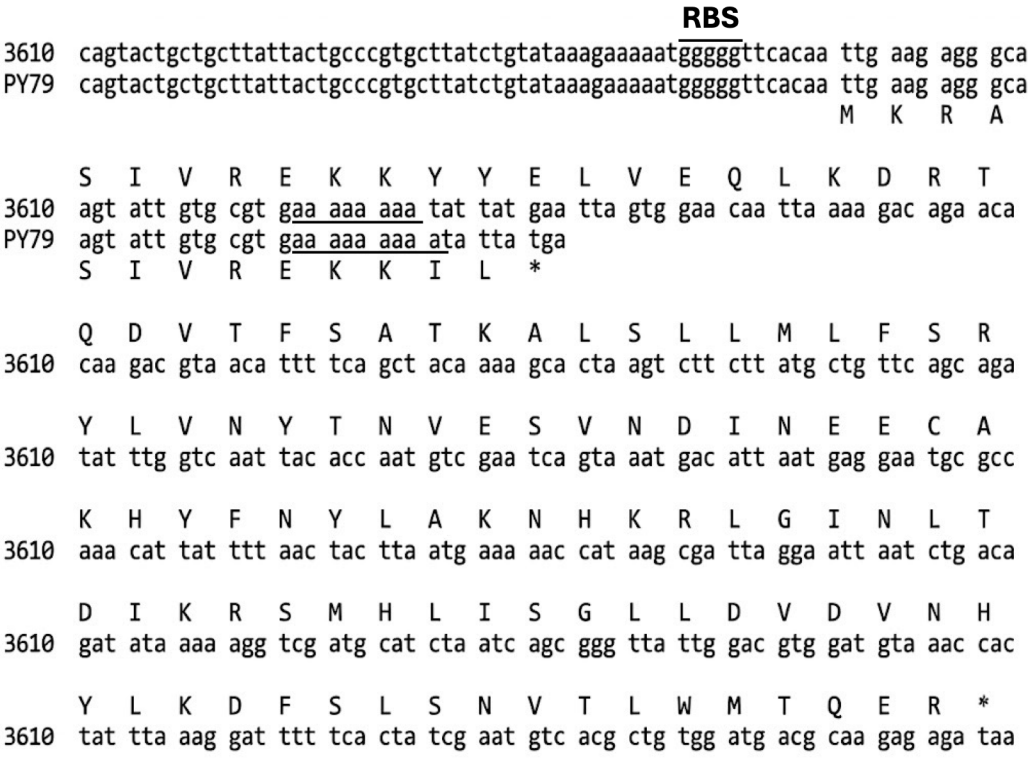

Figure 1.5. Sequence alignment of the *swrA* gene and amino acid sequence between wild-type *B. subtilis* (3610) and the laboratory strain PY79, adapted from [27]. Single-letter amino acid codes corresponding to strain 3610 are positioned above, whereas those for laboratory strains, as 168 or PY79, are positioned below. An insertion of an additional adenine in the homopolymeric tract of the domesticated strains introduces a frameshift mutation, leading to premature translation termination.

The expression of *swrA* is regulated by multiple promoters. Under growth in liquid medium, transcription is primarily driven by a σ^D-dependent promoter located upstream of the *swrA* coding region. SwrA promotes transcription of the *fla/che* operon, which includes *sigD*, thereby creating a positive feedback loop that further enhances *swrA* expression (Figure 1.6). In addition, a second promoter with features of a σ^A-dependent promoter can become active in the presence of DegU-P, which accumulates in the stationary phase. Thus, *swrA* expression can be influenced by both the σ^D regulatory network and DegU-P-dependent regulation, allowing its expression to respond to the physiological state of the cell [24,26].

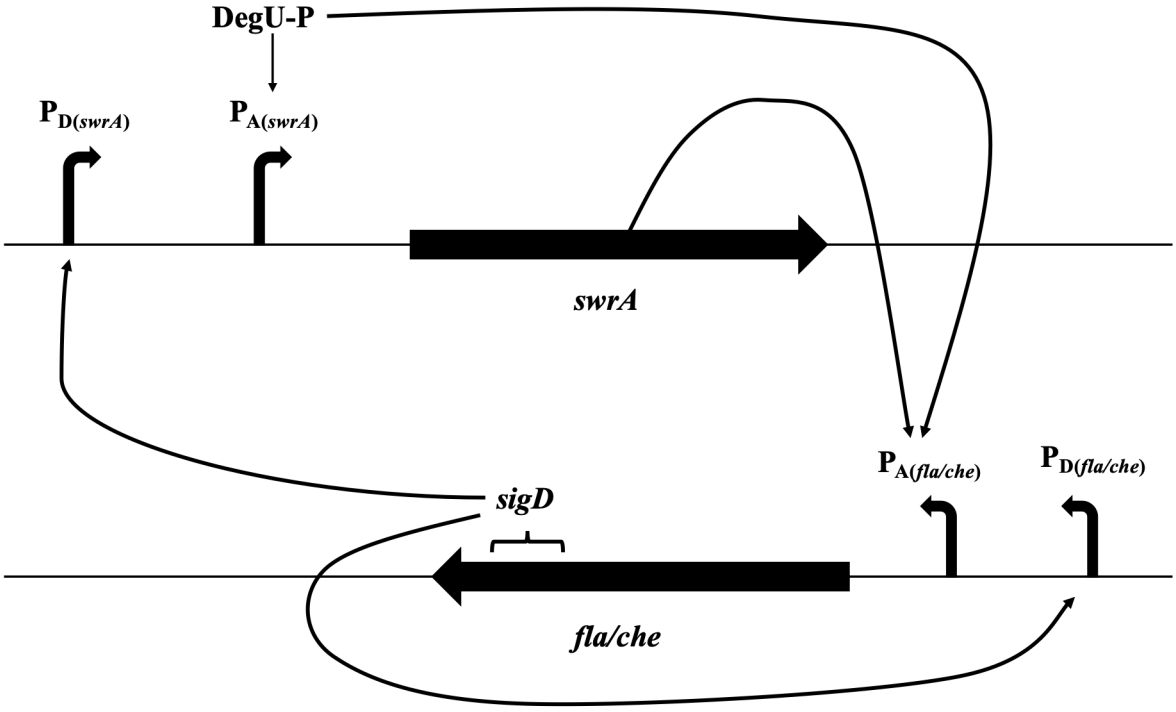

Figure 1.6. Schematic model of the multi-promoter regulation of *swrA* and its positive feedback loop with *sigD*, adapted from [26]. Expression of *swrA* is driven by two distinct promoters: a DegU-P-activated promoter $P_{A(swrA)}$ and a sigmaD-dependent promoter $P_{D(swrA)}$. Upon activation, SwrA induces the *fla/che* operon together with DegU-P, producing SigD and forming a positive feedback loop that drives *swrA* expression.

SwrA plays an important role in regulating *Bacillus subtilis* motility through its interaction with the DegS-DegU two-component system, being required for the increased flagellation necessary for swarming differentiation on solid surfaces [28]. At the *fla/che* promoter, DegU-P can function either as a transcriptional activator or repressor depending on the presence of functional SwrA: in a *swrA*$^+$ background, SwrA interacts with DegU-P and promotes transcription of the *fla/che*

operon, which is required for flagellar synthesis and motility. In contrast, in the absence of SwrA, DegU-P represses *fla/che* expression, resulting in loss of flagellar formation and motility. Importantly, the mutant protein DegU32(Hy)-P is impaired in its interaction with SwrA and therefore remains repressive at the *fla/che* promoter even in the presence of functional SwrA, while the presence of the *degS200(Hy)* allele, which increases the cellular level of wild-type DegU-P, does not prevent SwrA-dependent activation of *fla/che* [24].

Table 1.2 Effect of SwrA and DegU-P status on $P_{fla/che}$ regulation and motility in *B. subtilis*.

Strain / Background	***swrA* Status**	**$P_{fla/che}$ Regulation**	**Swimming**	**Swarming**
Wild type	*swrA*$^+$	Activated	Yes	Yes
ΔswrA	*swrA*$^-$	Basal	Reduced	No
degS200(Hy)	*swrA*$^+$	Activated	Yes	Yes
degS200(Hy)	*swrA*$^-$	Strongly repressed	No	No
degU32(Hy)	*swrA*$^+$ or *swrA*$^-$	Strongly repressed	No	No

In addition to transcriptional regulation, the cellular level of SwrA is also regulated in response to the growth environment. It was shown that the *swrA* gene is expressed in both liquid and solid media [28]. Subsequent studies revealed that this regulation also occurs at the protein level through controlled proteolysis. During growth in liquid medium, the adaptor protein SmiA promotes the degradation of SwrA by the LonA protease, limiting SwrA accumulation (Figure 1.7). This restricts hyperflagellation. Upon contact with a solid surface, SmiA-dependent proteolysis is relieved, allowing SwrA to accumulate and promote the expression of flagellar genes required for swarming [29,30]. Thus, SwrA abundance is regulated at both the transcriptional and post-translational levels, enabling its activity to respond to changes in the cellular environment.

SwrA also plays an important role in γ-PGA production by contributing to the activation of the *pgsBCAE* operon through its interaction with DegU-P. Both the *degU32(Hy)* and *degS200(Hy)* mutations are independently able to restore γ-PGA production in domesticated *B. subtilis* strains carrying a functional *swrA* allele. In the wild-type *degSU* background, *pgsBCA* is not expressed in the absence of *swrA* and is expressed only at trace levels in the *swrA*$^+$ strain [31].

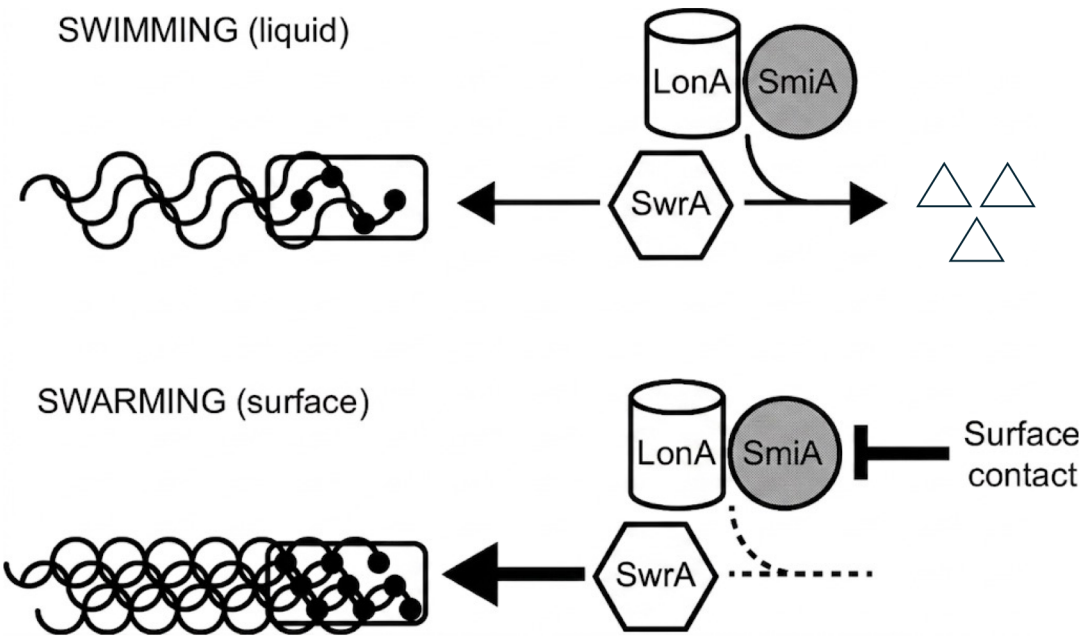

Figure 1.7. Post-translational control of SwrA levels in response to liquid and surface environments, reproduced from [29]. In liquid media, SmiA targets SwrA for degradation by the LonA protease. Upon surface contact, SmiA-dependent proteolysis is inhibited, allowing SwrA to accumulate and induce hyperflagellation.

Moreover, it was shown that the activation of the *pgs* operon has a different profile in *degU32(Hy)* and *degS200(Hy) swrA*$^{+}$ strains; expression is sustained until late stationary phase only in the presence of the *degS200(Hy)* allele [25]. These findings demonstrate that efficient γ-PGA production depends on the combined activity of DegU-P and SwrA, rather than on either regulator alone.

In contrast to its positive role in *pgsBCAE* and *fla/che* expression, SwrA can negatively regulate other DegU-P-dependent genes. SwrA has been shown to repress the expression of *aprE*, which encodes the extracellular protease subtilisin, and the production of cellulases and xylanases [25]. This illustrates that the regulatory outcome of DegU is influenced by its interaction with SwrA (Figure 1.8).

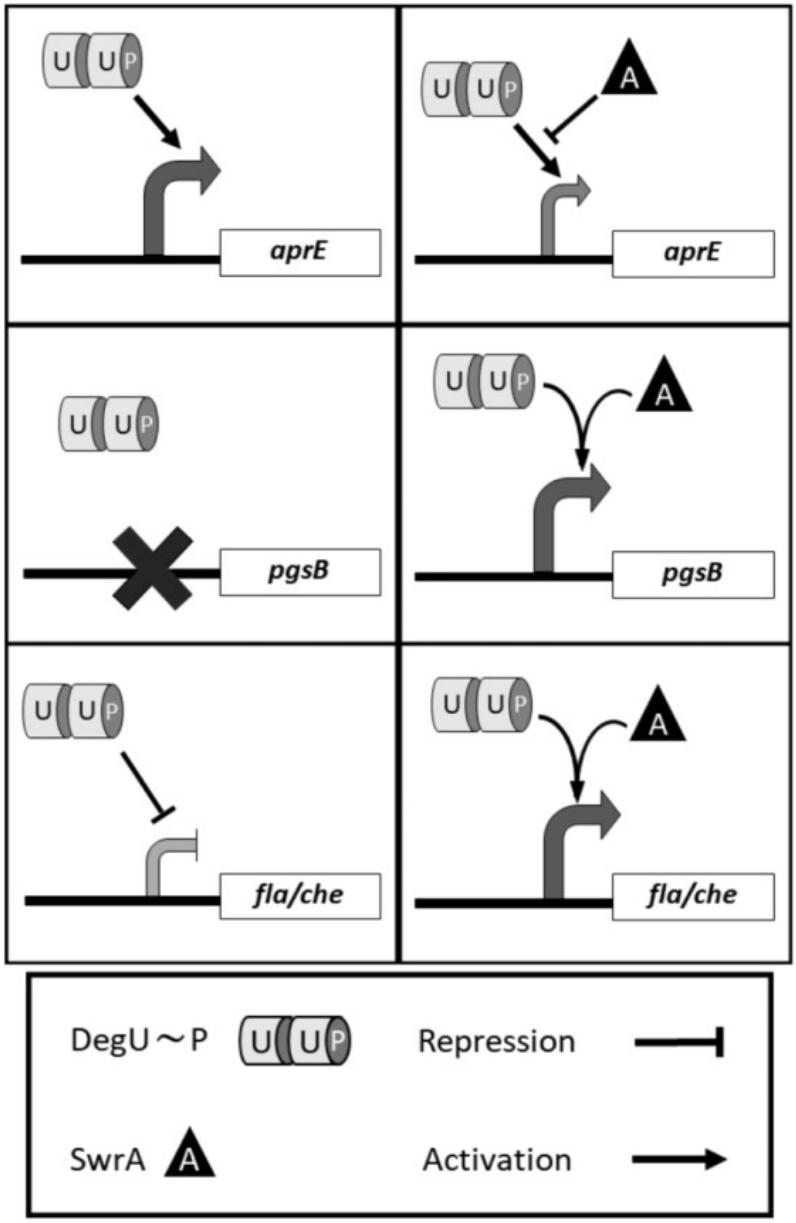

Figure 1.8. Dual regulatory role of SwrA as an activator and repressor of DegU-P target genes, reproduced from [25]. SwrA represses *aprE* expression while co-activating the *pgsBCAE* and *fla/che* operons.
SwrA also modulates DegU-P activity in the regulation of competence for DNA uptake. Although Hy mutations in *degU* or *degS* strongly impair competence, the presence of functional SwrA partially restores competence in the *degS200(Hy)* background. In contrast, SwrA does not restore competence in the *degU32(Hy)* background, consistent with the impaired interaction of the DegU32(Hy) protein with SwrA [25].

Beyond these roles, SwrA also influences biofilm development. A recent study showed that a frameshift mutation in *swrA* in a natural *B. subtilis* isolate resulted in altered macrocolony biofilm morphology, characterized by reduced structural complexity. This phenotype was reproduced in

independently constructed *swrA* disruption mutants, demonstrating that loss of functional SwrA can affect biofilm development. The altered biofilm morphology was proposed to result from downstream effects on extracellular matrix components, including exopolysaccharides and γ-PGA [32].

The mutation the frequently affects the *swrA* gene is considered a phase variation event. The *swrA* ORF contains an eight-adenine homopolymeric tract, which is prone to frameshift mutations. Frameshift mutations in this repeat have been estimated to occur at a frequency of 10^{-4} to 10^{-5}, approximately five orders of magnitude higher than the point mutation rate in *B. subtilis*, estimated at around 10^{-10} mutations per base pair per generation [27]. Loss of functional SwrA through such frameshift mutations has been shown to reduce *sigD* expression and, through lack of expression of *sigD*-dependent autolysins, promotes bacterial filamentation [33]. More recently, phase variation in *swrA* was shown to provide a selective advantage under protistan predation, as *swrA* frameshift mutants exhibiting filamentous morphology were consumed at a lower rate than wild-type cells [34]. These findings suggest that stochastic switching between functional and non-functional SwrA states may generate phenotypic heterogeneity and provide a bet-hedging strategy under different conditions.

Taken together, these studies highlight the diverse roles of SwrA, including the regulation of motility, γ-PGA production, competence, biofilm development, and other physiological processes. Despite the growing understanding of its functions, SwrA remains a relatively understudied regulatory protein, and many aspects of its regulation and biological functions remain to be fully understood. Further studies are therefore needed to better understand the molecular mechanisms governing SwrA activity and to clarify its broader role in bacterial physiology.

1.5 γ-PGA

Poly-γ-glutamic acid (γ-PGA) is a naturally occurring, biodegradable biopolymer composed of glutamic acid residues linked through γ-peptide bonds between the α-amino and γ-carboxyl groups. Depending on the producing organism and growth conditions, γ-PGA can consist of D-glutamic acid, L-glutamic acid, or a combination of both enantiomers. In *Bacillus subtilis*, γ-PGA is produced as an extracellular polymer and is an important component of the extracellular matrix. Due to its biodegradability, biocompatibility, water solubility, high water-absorption capacity, and

metal-chelating ability, γ-PGA has attracted considerable interest for applications in food, pharmaceutical, cosmetic, agricultural, and environmental industries [35].

In the food industry, γ-PGA can be used as a thickening and stabilizing agent to improve the texture and properties of food products and beverages. Its high water-retention capacity has also led to applications in cosmetics, where γ-PGA can function as a humectant and moisturizing agent. In pharmaceutical and biomedical applications, its biodegradability and biocompatibility make γ-PGA a promising material for drug and gene delivery systems. Its ability to bind metal ions and other compounds has additionally been exploited in wastewater treatment and environmental remediation, while its water-retention properties have potential applications in agriculture, including soil conditioning and seed coating. γ-PGA and its derivatives have also been investigated as biodegradable alternatives to conventional synthetic polymers [36].

In *Bacillus subtilis*, γ-PGA synthesis is mediated by the *pgsBCAE* operon, which encodes the components required for polymer synthesis and its transport across the cell membrane. PgsB, PgsC, and PgsA constitute the core γ-PGA synthetase complex, with PgsB functioning as the catalytic component responsible for polymerization of glutamate residues. PgsC is required for the activity of the synthetase complex, while PgsA is involved in the epimerization of L-glutamate into D-glutamate [37]. PgsE, encoded as the fourth gene of the operon, may form a complex with PgsA, although its precise function remains unclear. It has been shown that expression of *pgsBCA* alone is sufficient for γ-PGA production in transgenic tobacco plants [36]. In addition to its synthesis, γ-PGA levels are also influenced by its degradation. The *pgdS* and *ggt* genes, encoding a γ-PGA-specific hydrolase and the γ-glutamyl transferase, both contribute to the degradation of the polymer and can therefore affect the amount of γ-PGA accumulated extracellularly [39].

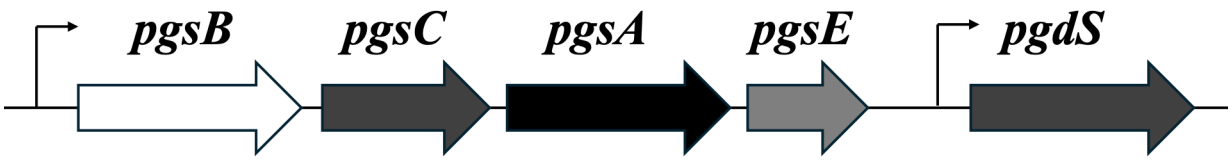

Figure 1.9. Genetic organization of the *pgsBCAE* operon and the downstream *pgdS* gene in *Bacillus subtilis*, adapted from [38].

Expression of the *pgsBCAE* operon is regulated by the DegS–DegU two-component system and the ComP–ComA quorum-sensing system. Under conditions of high cell density, phosphorylated

ComP transfers the phosphate group to ComA, generating ComA-P, which activates expression of *degQ*. DegQ then promotes phosphotransfer from DegS to DegU, leading to the accumulation of DegU-P. The level of DegU-P is an important determinant of *pgsBCA* expression, and deletion of *degQ* has been shown to markedly reduce γ-PGA production in *B. subtilis* [40].

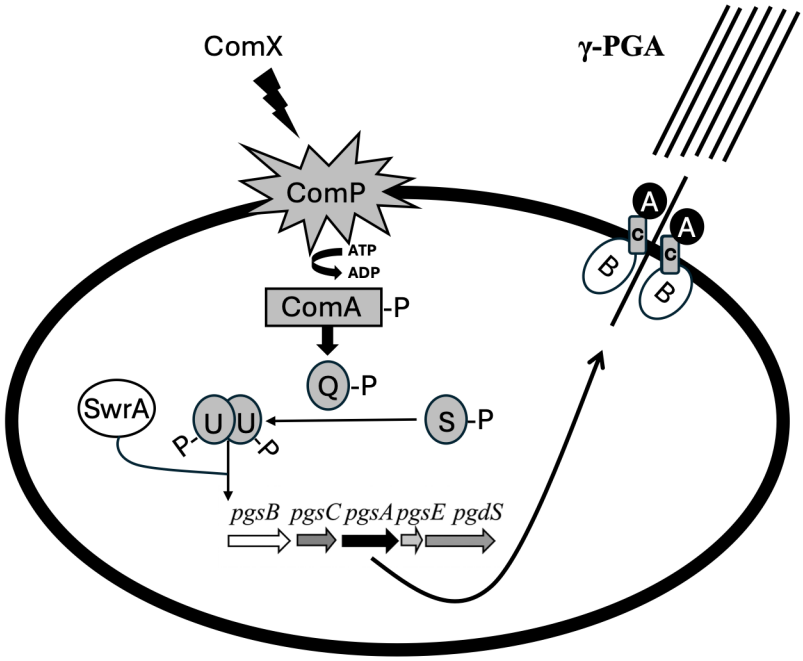

Figure 1.10. Regulatory network governing γ-PGA biosynthesis in *Bacillus subtilis*, adapted from [38].

Although the physiological functions of γ-PGA in *B. subtilis* are not fully understood, several roles have been proposed. γ-PGA has been shown to protect *B. subtilis* against zinc and copper intoxication, suggesting a role in resistance to metal stress [41]. In other bacteria, γ-PGA can have distinct physiological functions. For example, it forms a capsule in *Bacillus anthracis* that contributes to immune evasion and virulence, and it also contributes to immune evasion and persistence during infection in *Staphylococcus epidermidis* [42, 43].

In *B. subtilis*, γ-PGA has also been implicated in biofilm development. Although γ-PGA is not required for biofilm formation, it is shown that its production can increase the structural complexity and robustness of colony biofilms. Deletion of the *pgs* operon resulted in less structured and less robust colony biofilms in several environmental isolates, whereas increased γ-PGA production was associated with more complex biofilm architecture [44].

More recently, γ-PGA was shown to have an active role in biofilm dispersion. It is shown that in *B. subtilis* biofilms, motile cells located in the interior produce γ-PGA, which accumulates

extracellularly around these cells (Figure 1.11). Due to its polyanionic and hydrogel properties, γ-PGA can absorb water and swell, generating osmotic pressure within the biofilm. This swelling produces mechanical forces that push motile cells outward from the interior of the biofilm, resulting in localized cell ejection and dispersal. Consistent with this mechanism, deletion of the *pgsBCAE* operon did not prevent biofilm formation but abolished the localized dispersal phenotype, whereas increased γ-PGA production promoted extensive biofilm disruption [45]. These findings demonstrate that γ-PGA can influence not only the structure of *B. subtilis* biofilms but also their dynamics by providing a physical mechanism for cell dispersal.

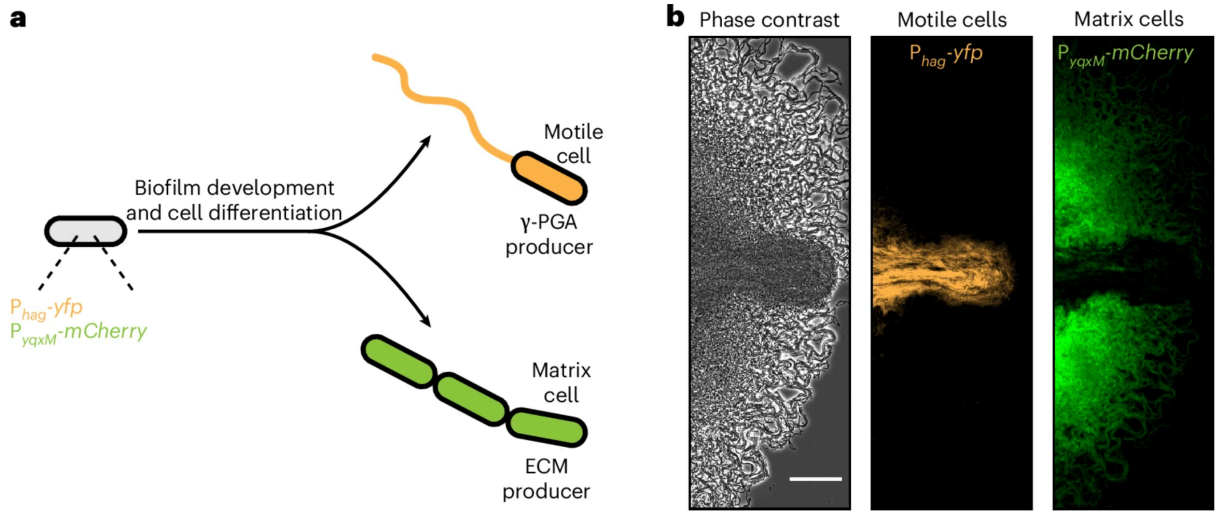

Figure 1.11 γ-PGA-mediated biofilm dispersal in *Bacillus subtilis*, reproduced from [45].
(a) Schematic representation of cell differentiation. (b) Microscopy images showing cell-specific expression of P_{hag}-*yfp* (motile cells) and P_{yqxM}-*mCherry* (matrix cells).

It has been shown that γ-PGA production is strongly influenced by temperature. In *B. subtilis* NCIB 3610, γ-PGA production was strongly reduced at temperatures below 37 °C, indicating that temperature is an important factor affecting γ-PGA biosynthesis [46]. Therefore, understanding how temperature influences the regulatory pathways controlling γ-PGA biosynthesis represents an important question, particularly regarding the factors regulating the expression of the *pgsBCA* operon.

1.6 RNA Thermometers

As a soil-dwelling bacterium, *Bacillus subtilis* is exposed to fluctuations in environmental temperature throughout its life cycle. Changes in temperature can affect fundamental cellular processes, including membrane fluidity, protein stability, metabolic activity, and the efficiency of gene expression. To maintain cellular function under changing conditions, bacteria must be able to sense temperature changes and rapidly adjust the expression of genes involved in adaptation. In addition to protein-based sensory and regulatory systems, temperature can be sensed directly through changes in the structure of RNA molecules. Such RNA-based regulatory elements, known as RNA thermometers, provide a rapid mechanism for controlling gene expression in response to temperature [47].

RNA thermometers are most commonly located within the 5′ untranslated regions of bacterial mRNAs, where their structures can regulate translation initiation. Temperature-dependent changes in RNA folding can be altered, thereby controlling translation without requiring an intermediate protein regulator (Figure 1.12). At lower temperatures, base pairing within the RNA can sequester the ribosome-binding site and prevent translation initiation, whereas increasing temperature can destabilize the structure and expose the ribosome-binding site, allowing translation to proceed [47,48].

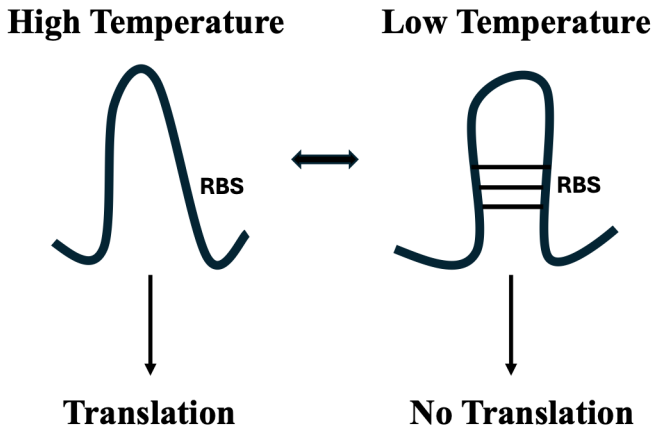

Figure 1.12. Schematic representation of an RNA thermometer mechanism.

RNA thermometers comprise a structurally diverse group of regulatory elements, ranging from relatively simple hairpin structures to more complex arrangements involving multiple stem-loops, pseudoknots, or other RNA–RNA interactions. Based on their mode of structural transition, they

have been broadly classified as zipper-like or switch-like thermometers. Zipper-like thermometers undergo progressive structural melting as temperature increases, whereas switch-like thermometers undergo a more pronounced transition between alternative RNA conformations (Figure 1.13) [48].

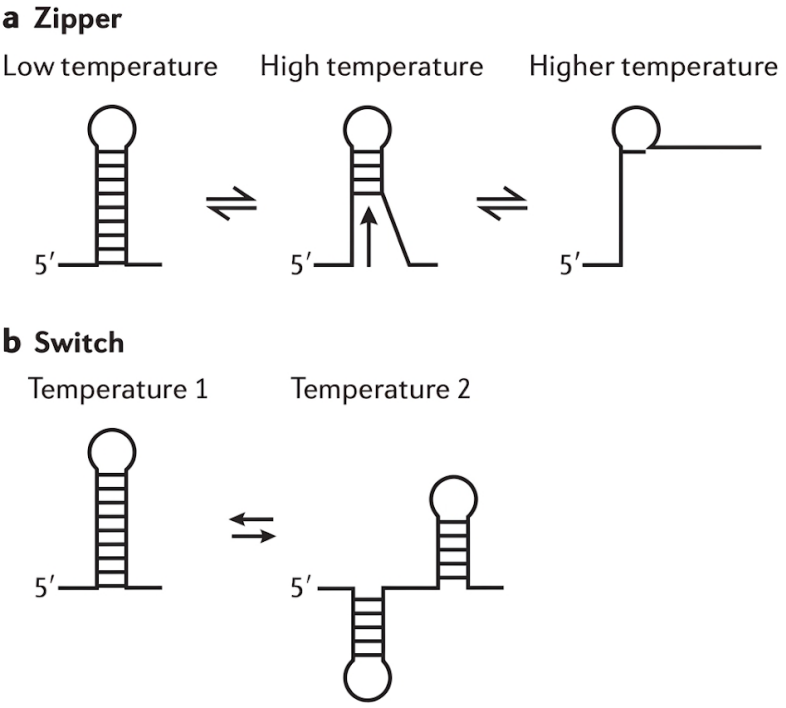

Figure 1.13. Zipper-like and Switch-like RNA thermometers, reproduced from [48]. (a) Zipper-like thermometers undergo melting as temperature increases. (b) Switch-like thermometers undergo a transition between different RNA conformations.

Several well-characterized RNA thermometers have been identified in bacteria, including the ROSE and FourU families. ROSE (Repression of Heat Shock Gene Expression) elements are typically located upstream of small heat-shock genes and consist of multiple hairpin structures. The most 3′ hairpin contains the ribosome-binding site and is specifically destabilized at elevated temperatures, allowing translation to increase. FourU elements are characterized by a stretch of four uridines that can base-pair with the AGGA sequence of the Shine–Dalgarno region. The best-characterized FourU thermometer is located upstream of the *agsA* gene in *Salmonella enterica*, where the temperature-dependent structure of the 5′ untranslated region regulates translation initiation [48].

Beyond the heat-shock response, RNA thermometers have also been identified in the regulation of virulence-associated genes in pathogenic bacteria. In *Yersinia pestis*, production of the virulence gene activator LcrF is substantially higher at 37 °C than at 26 °C despite similar levels of *lcrF* transcription. A similar mechanism regulates the virulence activator PrfA in *Listeria monocytogenes*, where a temperature-responsive RNA structure in the *prfA* leader regulates translation, resulting in increased PrfA production at higher temperatures [47, 49].

RNA thermometers are not restricted to sensing increases in temperature. Cold-responsive RNA thermometers have also been described and are associated with the regulation of genes involved in adaptation to low-temperature conditions. In contrast to many heat-responsive RNA thermometers, which have been extensively characterized, cold-responsive thermometers are less well understood and lack a conserved structural motif [47, 48].

RNA thermometers have been experimentally identified also in *Bacillus subtilis*. A recent transcriptome-wide analysis of RNA structure at different temperatures identified temperature-responsive RNA structures in the 5′ untranslated regions of *glpF* and *glpT*, which regulate translation of these glycerol permease genes in a temperature-dependent manner [50]. These findings demonstrate that RNA thermometers can regulate endogenous genes in *B. subtilis*. However, whether RNA thermometers are involved in the temperature-dependent regulation of γ-PGA production has not been established.

2.0 Aim of the Work

Poly-γ-glutamic acid (γ-PGA) is an extracellular polymer produced by *Bacillus subtilis* with diverse biological and biotechnological applications. Its production is regulated by the *pgs* operon, whose activation requires the response regulator DegU in its phosphorylated form (DegU-P) and the small regulatory protein SwrA. Although the temperature dependence of γ-PGA production has been observed, the molecular mechanisms underlying this regulation remain unclear.

The research problem addressed in this work was the molecular basis of the temperature-dependent regulation of γ-PGA biosynthesis. In particular, this study aimed to determine whether the reduced activation of the *pgs* operon at lower temperatures is associated with temperature-dependent regulation of *swrA* expression, with changes in DegU-P activity, or both.

To address this problem, the following specific objectives were pursued:

1. To characterize the effect of growth temperature (24 °C vs. 37 °C) on γ-PGA production and *pgsB* expression, using a P_{pgsB}-*sfGFP* transcriptional reporter.
2. To determine whether SwrA levels are affected by growth temperature, using a SwrA-YFP fusion protein, and whether this correlates with the observed changes in *pgsB* expression.
3. To assess DegU-P activity at each temperature using a P_{aprE}-*gfp* transcriptional reporter in a Δ*swrA* background, in order to evaluate the contribution of DegU-P to *pgsB* regulation independently of SwrA.

By dissecting the relative contributions of SwrA and DegU-P to the temperature sensitivity of *pgs* expression, this work aims to provide mechanistic insight into how *B. subtilis* links changes in growth temperature to γ-PGA biosynthesis, a regulatory connection that has not yet been characterized.

3.0 Materials and Methods

3.1 Bacterial Strains

Table 3.1. List of *B. subtilis* strains used in this work.

Strain	Genotype	Reference
PB5249	*pheA1, trpC2, swrA+*	[28]
PB5390	*pheA1, trpC2, swrA+, degS200(Hy)*; Sp	[32]
PB5470	*pheA1, trpC2,, ΔswrA (kan)*	Laboratory Collection
PB5723	*pheA1, trpC2, swrA+, P_{aprE}-gfp, degS200(Hy)*; Km, Cm, Sp	[25]
PB5725	*pheA1, trpC2, ΔswrA, P_{aprE}-gfp, degS200(Hy)*; Km, Cm, Sp	[25]
PB5745	*pheA1, trpC2, swrA+, ywsC::RBSspoVG:sfGFP_Phyperspank::ywsC, degS200(Hy)*; Em, Sp	[25]
PB5974	*pheA1, trpC2, swrA+, degS200(Hy), pJM114 PswrARBSwt*; Km, Em	This work
PB5975	*pheA1, trpC2, swrA+, degS200(Hy), pJM114 PswrARBSmut*; Km, Em	This work
PB5978	*pheA1, trpC2, swrA+, degS200(Hy), PKS::PswrARBSwt-swrA:yfp*; Cm, Sp	This work
PB5979	*pheA1, trpC2, swrA+, degS200(Hy), PKS::PswrARBSmut-swrA:yfp*; Cm, Sp	This work
PB5980	*pheA1, trpC2, ΔswrA, PKS::PswrARBSwt-swrA:yfp*; Cm, Km	This work
PB5981	*pheA1, trpC2, ΔswrA, PKS::PswrARBSmut-swrA:yfp*; Cm, Km	This work
PB5249+Shortissimo	*pheA1, trpC2, swrA+, PKS::PswrARBSwt-swrA(1-7):yfp*; Cm	This work

PB5390+Shortissimo	*pheA1, trpC2, swrA+, degS200(Hy), PKS::PswrARBSwt- swrA(1-7):yfp*; Cm, Sp	This work
PB5470+STlich	*pheA1, trpC2,, ΔswrA (kan), PKS::PswrARBSwt- swrASTlich:yfp*; Cm, Km	This work
PB5390+STlich	*pheA1, trpC2, swrA+, degS200(Hy), PKS::PswrARBSwt-swrASTlich:yfp*; Cm, Sp	This work

3.2 Plasmids

Table 3.2. List of plasmids used in this work.

Plasmid	**Genotype**	**Reference**
pJM114 SwrA TOT	*pJM114 PswrARBSwt-swrATOT*; Km	[26]
pJM114 SwrA TOT RBS mut	*pJM114 PswrARBSmut-swrATOT*; Km	Laboratory Collection
pIYFP	*bla, iyfp*; Cm	[51]
pHCMC05	Replicative vector; P_{spac} promoter; Cm	[52]
pSwrAA	*pHCMC05* P_{spac} *-swrA;* Cm	[26]
pSSC1	*pSB1AK3 PKS-PswrARBSwt-mCherry*; Km	Laboratory Collection
pSSC2	*pSB1AK3 PKS-PswrARBSmut-mCherry*; Km	Laboratory Collection
pSwrA-YFP	*pIYFP PswrARBSwt-swrA:yfp*; Cm	Laboratory Collection
pIYFP SwrA-YFP WT	*pIYFP PKS-PswrARBSwt-swrA:yfp*; Cm	This work
pIYFP SwrA-YFP MUT	*pIYFP PKS-PswrARBSmut-swrA:yfp*; Cm	This work
pIYFP STlich	*pIYFP PKS-PswrARBSwt-swrASTlich:yfp*; Cm	This work
pIYFP Shortissimo	*pIYFP PKS-PswrARBSwt-swrA(1-7):yfp*; Cm	This work

3.3 Primers

Table 3.3. List of primers used in this work.

Primer	Sequence
PKS+PromMut_fwd	AGGGAACAAAAGCTGGGTACGAATTCAACCAGTCTTTGC
PKS+PromMut_rev	TTGTGAACCCCCATTTTC
SwrA-YFP_fwd	GTGCTTATCTGTATAAAGAAAATGGGG
SwrA-YFP_rev	CTGCTTCATGTGGTCGGG
FoSTLICH	GAGAGAGAAAAAATACTATGAATTAGTGGAACAATTAAAAGACAG
ReSTLICH	GTATTTTTTCTCTCTCACAATACTTGCCCTCTTC
FwPA	CATTTATAAAGGACTGTTATTACCCG
T7	TAATACGACTCACTATAGGG
SwrA-Bsa_Rev	GGTCTCACCAACACAATACTTGCCCTCTTC
BsaI-FYFP	CGGTCTCCTTGGATTCAATAGAAAAGGTAAGC
Up2UpProm	TCGACACTCGCACTGCAGAGAC
pGEXinter	ACGGAATTCACTATCTCTCACCGCCTCAAGC
pks4check	TACTGATCAGGATTTGCACC
M13For 24mer	CGCCAGGGTTTTCCCAGTCACGAC
PKSfor	GGGAATTCGCTTACACCCTGCAGGTC
eGFP n	CGTCGCCGTCCAGCTCGACCAG
vzdF	CGGAATTCTAACGAGTTAATATGCA
RevPA2	CAGCTGCCATTAACCTGATTACTG
PREX4	TACTTGCCCTCTTCAATTGTGAACCCC
PREX97-122	CTGAACAGCATAAGAAGACTTAGTGC

3.4 Mediums and Buffers

Table 3.4. Composition of Luria-Bertani (LB) medium.

LB Component	Final Concentration
Tryptone	10 g/L
Yeast Extract	5 g/L
NaCl	10 g/L
Bacto™ Agar (only for solid medium)	15 g/L

When selection was required, media were supplemented with antibiotics at the following final concentrations:

- Ampicillin 100 µg/mL
- Chloramphenicol 5 µg/mL
- Kanamycin 2 µg/mL

To prepare LB medium for swarming assays, the final concentration of Bacto™ Agar was adjusted to 7 g/L.

Table 3.5. Composition of Tryptose Blood Agar Base (TBAB) (Antibiotic medium 3, DIFCO™) medium.

TBAB Component	Final Concentration
TBAB	33 g/L

When selection was required, media were supplemented with antibiotics at the following final concentrations:

- Chloramphenicol 5 µg/mL
- Kanamycin 2 µg/mL

Table 3.6. Composition of Double-Strength Schaeffer's-Glucose (2XSG) medium.

2XSG medium components	**Formula (stock)**	**Final concentration**
Nutrient Broth	DIFCO™ powder	16 g/L
Potassium Chloride	KCl (powder)	2 g/L
Magnesium Sulfate Heptahydrate	$MgSO_4 \cdot 7H_2O$ (powder)	0.5 g/L
Sodium Hydroxide	NaOH (1 M)	0.5 mL/L
After autoclaving and cooling to 50°C add:	-	-
Calcium Nitrate	$Ca(NO_3)_2$ (1 M)	1 mL/L
Manganese(II) Chloride	$MnCl_2$ (0.1 M)	1 mL/L
Iron(II) Sulfate	$FeSO_4$ (1 mM)	1 mL/L
Glucose	$C_6H_{12}O_6$ (50% w/v)	2 mL/L

Table 3.7. Composition of Super Optimal Broth with Catabolite Repression (SOC) medium.

SOC medium components	**Formula (stock)**	**Final concentration**
Tryptone	DIFCO™ powder	20 g/L
Yeast Extract	DIFCO™ powder	5 g/L
Sodium Chloride	NaCl (powder)	0.58 g/L
Potassium Chloride	KCl (powder)	0.18 g/L
Magnesium Sulfate Heptahydrate	$MgSO_4 \cdot 7H_2O$ (powder)	2.46 g/L
Magnesium Chloride	$MgCl_2$ (powder)	2.04 g/L
After autoclaving and cooling to 50°C add:		
Glucose	$C_6H_{12}O_6$ (50% w/v)	7.2 mL/L

Note: Super Optimal Broth (SOB) was prepared according to the formulation in Table 3.7, excluding the addition of glucose.

Table 3.8. Composition of Phosphate-Citrate (PC)10X buffer (pH=7).

PC 10X buffer components	**Formula (stock)**	**Final concentration**
Dipotassium Phosphate	K_2HPO_4	107 g/L
Monopotassium Phosphate	KH_2PO_4	60 g/L
Trisodium Citrate Dihydrate	$Na_3C_6H_5O_7 \cdot 2H_2O$	8.45 g/L

Table 3.9. Composition of Minimal Defined (MD) medium.

MD medium components	Formula (stock)	Final concentration
PC buffer	10X (pH 7.0)	1X
Glucose	$C_6H_{12}O_6$ (50% w/v)	40 mL/L
Potassium aspartate	40% w/v	25 mL/L
Ferric ammonium citrate	2.2 mg/mL	5 mL/L
Magnesium sulfate	$MgSO_4$ (1 M)	3 mL/L
L-Phenylalanine	Phe (5 mg/mL)	10 mL/L
L-Tryptophan	Trp (5 mg/mL)	10 mL/L

MD medium was prepared under sterile conditions; stock solutions were autoclaved or filter-sterilized prior to mixing.

Luria-Bertani medium with magnesium (LM medium) was prepared by supplementing LB broth with $MgSO_4$ to a final concentration of 3 mM.

Table 3.10. Composition of Saline-Sodium Citrate (SSC) 20X buffer (pH=7).

SSC 20X buffer components	Formula (stock)	Final concentration
Sodium chloride	NaCl	175.3 g/L (3 M)
Trisodium citrate dihydrate	$Na_3C_6H_5O_7 \cdot 2H_2O$	88.2 g/L (300 mM)

Table 3.11. Composition of Tris-EDTA (TE) 1X (pH=8) Buffer

Components	Concentration
Tris base	10 mM
EDTA	1 mM

3.5 *E. coli* Transformation

Chemically competent *E. coli* TOP10 cells were retrieved from storage at -80 °C and thawed gently on ice. Under sterile conditions, the cells were dispensed into 50 µL aliquots for each transformation reaction.

Plasmid DNA (2–3 ng, in a total volume not exceeding 5 µL) was added to the cells, and the mixture was incubated on ice for 10 minutes.

Heat shock was performed in a water bath at 42 °C for 90 seconds, after which the samples were immediately returned to ice.

Nine volumes of SOC medium were added to the tube of competent cell volume (450 µL per 50 µL aliquote). The heat-shocked *E. coli* cells were incubated at 37°C for 30–45 minutes to allow for cell recovery.

The transformed cells were plated onto LB agar plates supplemented with ampicillin and incubated overnight at 37°C. The following morning, colony PCR was performed to screen for positive transformants.

3.6 *E. coli* Colony PCR

Colony PCR reactions were carried out using EmeraldAmp® GT PCR Master Mix (2X), containing the DNA polymerase, reaction buffer, dNTPs, and magnesium chloride. To provide the DNA template, single bacterial colonies were picked using a sterile micropipette tip and transferred directly into the reaction mixture (Table 3.12).

Table 3.12. The *E. coli* colony PCR reaction mixture.

Components	**Final concentration**
EmeraldAmp® GT PCR Master Mix 2X	1X
Forward primer	0.2 µM
Reverse primer	0.2 µM
Template DNA	Single bacterial colony

Table 3.13. Thermal cycling parameters for *E. coli* colony PCR.

Temperature	Time	
94 °C	8 minutes	
94 °C	20 seconds	25-30 Cycles
Annealing Temperature Dependent on primer T_m	30 seconds	
72 °C	1 minute/kb	
72 °C	5 minutes	
4 °C	∞	

3.7 Mini-Prep Plasmid Extraction from *E. coli*

The PCR-verified colony was inoculated into 3 mL of LB medium containing ampicillin and incubated overnight at 37 °C with orbital shaking. The bacterial culture was centrifuged at 14,000 rpm for 1 minute, and the supernatant was discarded. Plasmid DNA was extracted from PCR-positive *E. coli* colonies using the E.Z.N.A.® Plasmid DNA Mini Kit I (Omega Bio-tek) according to the manufacturer's instructions.

The cell pellet was thoroughly resuspended in 250 µL of Solution I supplemented with RNase A. The suspension was then transferred to a new 1.5 mL microcentrifuge tube.

Solution II (250 microliters) was added, and the tube was gently inverted several times to obtain a clear lysate. Lysis was limited to a maximum of 5 minutes.

Solution III (350 µL) was added immediately, and the tube was inverted several times until a white precipitate formed.

The mixture was centrifuged at 14,000 rpm for 10 minutes to yield a compact white pellet. The supernatant was carefully loaded onto the HiBind DNA Mini Column (around 700 µL) and centrifuged at 14,000 rpm for 1 minute. The flow-through was discarded.

HBC Buffer with isopropanol (500 µL) was added to the column and centrifuged at 14,000 rpm for 1 minute. The flow-through was discarded.

DNA Wash Buffer with ethanol (700 µL) was added to the column and centrifuged at 14,000 rpm for 30 seconds. The flow-through was discarded.

The empty column was centrifuged at 14,000 rpm for 2 minutes. The flow-through was discarded.

The column was transferred to a new 1.5 mL microcentrifuge tube, and 50 µL of Elution Buffer

was added. The mixture was incubated for 3 minutes at room temperature, followed by centrifugation at 14,000 rpm for 1 minute to elute the plasmid DNA. The eluted DNA was stored at -20 °C for subsequent analysis.

3.8 Rolling Circle Amplification (RCA)

RCA was utilized to facilitate the transformation of *Bacillus subtilis*. Amplification reactions were performed using the EquiPhi29 DNA Polymerase Kit (Thermo Scientific) according to the following protocol:

Table 3.14. Denaturation reaction formulation.

Component	**Volume**
EquiPhi29 DNA Polymerase Reaction Buffer (10X)	0.5 µL
Exo-Resistant Random Primers (100 µM)	1 µL
Template DNA	1 pg – 1 ng
Deionized Water	Brought to 5 µL

The mixture was adjusted to a final volume of 5 µL with deionized water, incubated at 95°C for 3 minutes in a thermocycler, and immediately transferred to ice for 5 minutes.

Table 3.15. RCA reaction formulation.

Component	**Volume**
Denatured DNA Mixture	5 µL
EquiPhi29 DNA Polymerase Reaction Buffer (10X)	1.5 µL
DTT (0.1 M)	0.2 µL
dNTP Mix (10 mM each)	2 µL
EquiPhi29 DNA Polymerase (10 U/µL)	1 µL
Deionized Water	Up to 20 µL

The total volume was brought to 20 µL with deionized water. The reaction mixture was incubated at 45°C for 3 hours, after which the polymerase was heat-inactivated at 65°C for 10 minutes.

3.9 *B. subtilis* Transformation

Competent *Bacillus subtilis* cells were prepared using a two-step growth protocol as follows:
The designated *B. subtilis* strain was inoculated from selective agar plates into 10 mL of LM medium and incubated at 37 °C in an orbital shaking water bath until reaching an optical density at 600 nm (OD_{600}) of 1.0 (approximately 2 hours).
The culture was diluted 1:20 by transferring 500 µL into 10 mL of MD medium. The culture was incubated at 37 °C with orbital shaking for 4 hours to allow the cells to reach stationary phase and enter a competent state.
Two aliquots of 500 µL of fresh competent cells were immediately set aside: one for the transformation reaction and one to serve as a negative control. The remaining 9 mL of culture was harvested by centrifugation at 4,000 rpm for 8 minutes. A volume of 5.4 mL of the supernatant was discarded, leaving 3.6 mL of culture. The cell pellet was thoroughly resuspended in this remaining 3.6 mL volume, and 400 µL of sterile 100% glycerol was added to yield a final 10% concentration suitable for cryopreservation. The resulting glycerol mixture was dispensed into 1.8 mL aliquots, labeled, and stored in liquid nitrogen for future transformations.
RCA product in a volume of 5 to 10 µL was added to a 500 µL aliquot of competent cells. A separate 500 µL aliquot received no DNA to serve as a negative control. Both mixtures were incubated at 37°C for 90 minutes in a shaking water bath to facilitate DNA integration.
The transformation mixtures were spread onto TBAB plates containing the appropriate selective antibiotic and incubated overnight at 37°C. Antibiotic-resistant transformants were subsequently verified by colony PCR.

3.10 *B. subtilis* Colony PCR

Individual bacterial colonies were picked from selective plates, resuspended in 30 µL of deionized water, and incubated at 100°C for 3 minutes to disrupt the cell wall and release template DNA. The cell suspension was centrifuged at 14,000 rpm for 3 minutes to pellet cellular debris. 3 µL vof the cleared supernatant was added to the PCR reaction mixture to serve as the DNA template (Table 3.16).

Table 3.16. Composition of the *Bacillus subtilis* colony PCR reaction mixture.

Components	**Final concentration**
EmeraldAmp® GT PCR Master Mix 2X	1X
Forward primer	0.2 µM
Reverse primer	0.2 µM
Lysate Supernatant (Template DNA)	3 µL

Table 3.17. Thermal cycling parameters for *Bacillus subtilis* colony PCR.

Temperature	**Time**	
94 °C	5 minutes	
94 °C	20 seconds	25-30 Cycles
Annealing Temperature Dependent on primer T_m	30 seconds	
72 °C	1 minute/kb	
72 °C	5 minutes	
4 °C	∞	

3.11 *B. subtilis* Genomic DNA Isolation

Genomic DNA was extracted from *Bacillus subtilis* cultures using an enzymatic lysis and chloroform-ethanol precipitation method. A 1.5 mL volume of bacterial culture was harvested by centrifugation at 14,000 rpm for 5 minutes, after which the supernatant was discarded.

The cell pellet was thoroughly resuspended in 275 µL of 1X SSC buffer containing 10 mg/mL lysozyme and incubated at 37 °C for 30 minutes to digest the peptidoglycan cell wall.

Following initial lysis, 84 µL of a 5 mg/mL pronase solution (pre-incubated at 37 °C for 30 minutes in 1X SSC buffer) and 100 µL of Dupanol solution were added to the sample.

The mixture was incubated at 60°C in a water bath with occasional inversion until the solution became clear. To remove proteins, 500 µL of chloroform was added and mixed thoroughly by gentle inversion, followed by centrifugation at 14,000 rpm for 3 minutes.

Approximately 400 µL of the upper aqueous phase was carefully transferred to 2.5 volumes of 100% ethanol to precipitate the genomic DNA.

The precipitated DNA was collected using a framed Pasteur pipette, washed in 70% ethanol, air-dried completely, and finally resuspended in 100 µL of 0.1X TE buffer for storage.

3.12 Site-Directed Mutagenesis

Site-directed mutagenesis was performed using an optimized protocol adapted from the QuikChange II Site-Directed Mutagenesis Kit (Agilent Technologies).
Mutagenic PCR reactions were prepared in a final volume of 10 µL according to the formulation in Table 3.18.

Table 3.18. Optimized site-directed mutagenesis reaction formulation.

Component	**Final Concentration / Volume**
Plasmid Template DNA	10 ng
Reaction Buffer S (10X)	1X
dNTP Mix (10 mM)	0.2 µL
Forward Primer (20 µM)	0.2 µL
Reverse Primer (20 µM)	0.2 µL
ChromoPFU	0.5 U
Deionized Water	Up to 10 µL

Amplification was carried out using a two-phase thermal cycling setting to maximize primer binding efficiency and specific amplification, as detailed in Table 3.19.

Table 3.19. Thermal cycling parameters for site-directed mutagenesis.

Temperature	**Time**
95°C	2 minutes
5 cycles of:	**1st Step:**
95°C	30 seconds
Primer Tm - 5°C	1 minute
72°C	1 minute/kb
20 cycles of:	**2nd Step:**
95°C	30 seconds
Primer Tm	1 minute
72°C	1 minute/kb
72°C	7 minutes
4°C	∞

Following thermal cycling, 0.5 µL of *Dpn*I (10 U/µL) restriction enzyme was added directly to the 10 µL PCR reaction mixture. The sample was gently mixed, and incubated at 37°C for 1 hour to digest methylated non-mutated template DNA. *Dpn*I-treated reaction was transformed into competent *E. coli* cells, followed by recovery and plating on selective media for mutant screening.

3.13 Gibson Assembly

Purified DNA inserts and linearized vector backbone were combined at an optimal molar ratio of 1:2 to 1:3 (vector-to-insert), maintaining a total DNA amount of less than or equal to 0.200 pmol. The DNA mixture was added to 2X GeneArt™ Gibson Assembly HiFi Master Mix, as detailed in Table 3.20.

Table 3.20. GeneArt™ Gibson Assembly HiFi reaction formulation.

Component	**Volume / Quantity**
Vector and Insert DNA	≤ 0.200 pmol total
GeneArt™ Gibson Assembly HiFi Master Mix (2X)	5 µL
Nuclease-Free Water	Up to 10 µL

The assembly reaction mixture was incubated at 50 °C in a thermal cycler for 30 minutes. Following incubation, the unpurified assembly mixture was transformed into competent *E. coli* cells, followed by recovery and plating on selective antibiotic media for mutant screening.

3.15 Plasmid Construction

pIYFP SwrA-YFP WT/MUT:

Recombinant plasmids pIYFP SwrA-YFP WT and pIYFP SwrA-YFP MUT were constructed using Gibson Assembly according to the following procedure:

The vector backbone was prepared by digesting the pIYFP plasmid with restriction enzymes *PstI* and *KpnI*. To eliminate background colonies originating from undigested parental plasmid, the linearized backbone was further digested with *HindIII*, a restriction site present within the excised insert region but absent from the final vector backbone.

The wild-type *PKS-PswrARBSwt* fragment was PCR-amplified using primer set PKS+PromMut_fwd and PKS+PromMut_rev using pSSC1 as the template DNA. The mutated *PKS-PswrARBSmut* fragment was amplified with the same primer pair using pSSC2 as the template DNA.

The *swrA-yfp* fragment was PCR-amplified using primer set SwrA-YFP_fwd and SwrA-YFP_rev using pSwra-YFP as the template DNA.

The prepared vector backbone, Fragment 1 (wild-type or mutant promoter), and Fragment 2 were joined by Gibson Assembly under the conditions detailed in Section 3.13, to create pIYFP SwrA-YFP WT and pIYFP SwrA-YFP MUT plasmids.

pIYFP STlich

The recombinant plasmid pIYFP STLich was generated via site-directed mutagenesis using pIYFP SwrA-YFP WT as the template plasmid. Mutagenic PCR was performed using the primer pair FoSTLICH (forward) and ReSTLICH (reverse) according to the reaction formulation and two-phase thermal cycling parameters described in Section 3.12.

pIYFP Shortissimo

The recombinant plasmid pIYFP Shortissimo was constructed using a combination of restriction-digestion and Gibson Assembly with the pIYFP SwrA-YFP WT plasmid serving as the template backbone.

First, two separate fragments were amplified from the template: the P_{swrA} promoter combined with the sequence encoding the first fifteen amino acids of swrA was amplified using primers FwPA and SwrA-Bsa_Rev, and the YFP sequence was amplified using primers BsaI-FYFP and T7. Both PCR products were digested with BsaI and ligated together, creating P_{swrA}- $swrA_{1-15}$-*yfp*.

Following verification that the two distinct fragments were successfully joined, the ligation product was re-amplified using primers FwPA and T7.

Simultaneously, the pIYFP SwrA-YFP WT vector backbone was linearized via double digestion with restriction enzymes *EcoRV* and *BstXI*.

Finally, the linearized vector backbone and the amplified insert fragment were joined by Gibson Assembly under the conditions detailed in Section 3.13.

3.16 Strain Construction

Strains PB5974 and PB5975, carrying the *swrA* wild-type and RBS-mutant alleles under their native promoter, were constructed by transforming strain PB5390 with plasmids pJM114 SwrA TOT and pJM114 SwrA TOT RBS mut, respectively, followed by selection on kanamycin-containing media.

Strains PB5978 and PB5979 were generated by transforming PB5390 with plasmid pIYFP SwrA-YFP WT and pIYFP SwrA-YFP MUT, respectively, integrating the $P_{swrA(RBSwt)}$-*swrA*:*yfp* fusion at the PKS locus. Strains PB5980 and PB5981 were constructed analogously by transforming strain PB5470 with pIYFP SwrA-YFP WT and pIYFP SwrA-YFP MUT, respectively, yielding the corresponding *swrA*:*yfp* fusions in the Δ*swrA* background carried by PB5470, with transformants selected on chloramphenicol-containing media.

Transformation with pIYFP-STLich yielded strains in both the PB5390 and PB5470 backgrounds, named PB5390 + STLich and PB5470 + STLich, respectively. Transformation with pIYFP-Shortissimo yielded strains in the PB5390 and PB5249 backgrounds, named PB5390 + Shortissimo and PB5249 + Shortissimo, respectively. All transformants were selected on chloramphenicol-containing media.

Following transformation, correct plasmid integration into the *pks* locus was verified by colony PCR. Since integration could potentially also occur within the *swrA* locus, both the *pks* and *swrA* regions were examined to confirm that integration occurred specifically at the *pks* locus.

For verification of the *swrA* locus, the primers Up2UpProm and pGEXinter were used, with amplification expected only in the absence of integration at the *swrA* locus. For verification of the *pks* locus, the primers pks4check and M13For 24mer were used, with amplification occurring only when integration had occurred at the *pks* locus.

Once colonies with confirmed integration at the *pks* locus were identified, genomic DNA was isolated and PCR was performed to amplify the region between the PKSfor and eGFP n primers for sequencing. The resulting PCR product was sequenced to verify the absence of unintended mutations.

Following sequence verification, a swarming assay was performed to collect $swrA^+$ cells. Colony expansion was visible after approximately 4 hours of incubation at 37 °C, and cells from the colony edges were collected, where they are expected to be predominantly $swrA^+$. The collected cells were inoculated onto 2xSG medium slants and incubated overnight with a loose cap. The slants were then tightly closed to limit oxygen access and promote sporulation, and stored at 4 °C for subsequent experiments.

3.16 Growth Assay and Fluorescence Measurement

Spores were first resuspended in a small volume of LB broth and thoroughly mixed to obtain a homogeneous suspension. The spore suspension was then equally distributed into the designated volumes of LB broth for each biological replicate.

For cultures grown at 37 °C, the assay was initiated in the morning. After approximately 2 hours of incubation, the first reliable optical density at 600 nm (OD_{600}) measurement was obtained ($OD_{600} > 0.1$). OD_{600} was subsequently measured at 30-min intervals, and a growth curve was generated to determine the transition from the logarithmic growth phase to the stationary phase. T_0 was defined as the turning point from the logarithmic phase to the stationary phase, and samples were collected two hours later (T_2) for fluorescence measurement.

For cultures grown at 24 °C, two separate growth curves were initially performed due to the slower growth rate in order to obtain the full growth profile. One growth curve was performed during the day and the other was started in the evening and run overnight to be monitored the following

morning. Based on the resulting growth profile, subsequent assays were started overnight and monitored the following morning. The first meaningful OD_{600} measurement was obtained after approximately 10 hours of incubation, after which OD_{600} was measured at 1-h intervals.

At T_2, cultures were harvested at an OD_{600} of approximately 0.75. The cell cultures were centrifuged, and the supernatant was removed to eliminate LB components that could contribute to background fluorescence. The cell pellets were washed twice with physiological saline solution (0.9% NaCl) and finally resuspended in 200 µL of 0.9% NaCl. The cell suspensions were then transferred to a 96-well plate for fluorescence measurement.

Fluorescence and OD_{600} measurements were performed using a Tecan Infinite M Plex 200 microplate reader, with fluorescence read from the top of the plate. Before each measurement, the plate was shaken linearly at an amplitude of 3.5 mm for 30 seconds to resuspend and homogenize the cell suspension. For GFP measurements, excitation and emission wavelengths were set to 480 nm and 530 nm, respectively, with a gain of 141. For YFP measurements, excitation and emission wavelengths were set to 510 nm and 550 nm, respectively, with a gain of 170. The same settings were used for all measurements. Fluorescence values were then blanked using the normalized fluorescence intensity of the corresponding non-fluorescent negative control, and OD_{600} was blanked using the resuspension solution. Fluorescence intensity was normalized to the corresponding OD_{600} measurement obtained from the microplate reader.

3.17 Overexpression of SwrA and PgsB for γ-PGA Production

PB5390 (*degS200Hy, swrA+*) and PB5745 (*degS200Hy, swrA+, $P_{hyper\text{-}spank}$-pgsB*) were transformed with either pHCMC05, the empty vector, or pSwrAA, carrying $P_{hyper\text{-}spank}$-*swrA* to create four different expression systems:

1. Overexpression of *pgsB*, as the positive control
2. Overexpression of *pgsB* and *swrA*
3. Overexpression *swrA*
4. Negative control with the empty pHCMC05.

Transformants were selected on TBAB agar supplemented with chloramphenicol. Since pHCMC05 and pSwrAA are replicative plasmids, chloramphenicol selection was maintained during subsequent growth. Each transformant was inoculated onto LB agar supplemented with

chloramphenicol and 0.5 mM IPTG and incubated for 16 h at 37 °C or 40 h at 24 °C. Following incubation, γ-PGA production was assessed and compared between the different strains.

3.18 RNA Isolation from *Bacillus subtilis*

Total RNA was extracted from *B. subtilis* strains PB5980, PB5470 + STlich, and PB5249 + Shortissimo, collected at T2 as previously described.

Cultures were harvested using the QIAGEN RNeasy Mini Kit with the RNase-Free DNase Set, following a protocol optimized for the thick stationary-phase cell wall.

A 5 mL aliquot of culture was harvested by centrifugation at 5,000 rpm for 5 minutes at 4 °C, and the supernatant was discarded completely.

The cell pellet was resuspended in 100 µL of freshly prepared enzymatic lysis buffer (TE buffer, pH 8.0, containing 50 mg/mL lysozyme) by thorough pipetting and incubated at 37 °C for exactly 15 minutes, during which the solution changed from opaque to slightly cleared/viscous. Immediately following incubation, the tube was subjected to a thermal shock by freezing in liquid nitrogen and then transferring to a 37 °C water bath until just thawed, to maximize cell lysis and RNA yield.

Following lysis, 350 µL of Buffer RLT (containing 10 µL β-mercaptoethanol per mL) was added to inactivate RNases, and the mixture was vortexed thoroughly.

Ice-cold ethanol (250 µL, 96–100%) was added to the lysate and mixed by pipetting.

The entire mixture (~700 µL) was loaded onto an RNeasy Mini spin column and centrifuged for 15 seconds at 13,000 rpm, discarding the flow-through.

The column was washed twice with 350 µL Buffer RW1, with each wash followed by centrifugation for 15 seconds at 13,000 rpm. It was followed by two washes with 500 µL Buffer RPE (15 seconds and 2 minutes, respectively, at 13,000 rpm), the latter to ensure complete removal of residual ethanol. The column was transferred to a new collection tube and centrifuged at full speed for 1 minute to dry the membrane.

RNA was eluted by transferring the column to a clean, RNase-free 1.5 mL microcentrifuge tube, applying 30–50 µL RNase-free water directly to the membrane, incubating at room temperature for 1 minute, and centrifuging for 1 minute at 13,000 rpm.

RNA quality and purity were assessed by spectrophotometry using a standard UV-Vis spectrophotometer, with A260/A280 and A260/A230 ratios of ≥2.0 and ≥1.5, respectively, taken

to indicate acceptable purity with minimal protein, lysozyme, or guanidine/ethanol contamination. Purified RNA was stored immediately at −20 °C.

3.19 Reverse Transcription PCR (RT-PCR)

To eliminate genomic DNA contamination prior to reverse transcription, total RNA was treated with DNase I and purified by ethanol precipitation.

A 15 µL reaction mixture was prepared by combining 10 µL of total RNA, 1.5 µL of 10× DNase buffer, 1 µL of DNase I enzyme, and 2.5 µL of nuclease-free water. The mixture was incubated at room temperature for 15 minutes. To terminate the enzymatic reaction, 1.5 µL of EDTA was added, and the sample was incubated at 65 °C for 10 minutes for heat inactivation.

The treated RNA was precipitated by adding 5 µL of 10 M ammonium acetate and 50 µL of ice-cold 100% ethanol. The sample was incubated at −80 °C for 10 to 15 minutes to facilitate precipitation, then centrifuged 13,000 rpm for 15 minutes. The supernatant was carefully removed, and the tube was briefly centrifuged to remove any remaining liquid completely. The resulting RNA pellet was resuspended in 5 µL of nuclease-free water.

Complementary DNA (cDNA) synthesis was performed on the purified RNA using strain-specific primer pools mixed in equimolar amounts. For Shortissimo (PB5249 + Shortissimo) samples, the primer mix comprised eGFP n, RevPA2, and SwrA-Bsa_Rev. For STlich (PB5470 + STlich) and PB5980 samples, the primer mix contained eGFP n, RevPA2, PREX4, and PREX97-122.

First, 2 µL of RNA was mixed with 2 µL of nuclease-free water (5 µL total volume) and incubated at 65 °C for 5 minutes in a thermocycler to melt secondary structure, followed by immediate transfer to ice.

A 6 µL master mix containing 1 µL dNTPs (25 mM stock; 1 mM final concentration), 2 µL of 5X reaction buffer (1X final concentration), 1 µL of the strain-specific primer mix, 1 µL RNase inhibitor (RNasin), and 1 µL reverse transcriptase enzyme was added, bringing the total reaction volume to 10 µL.

The reaction was mixed thoroughly and incubated at 50 °C for 45 minutes for reverse transcription, followed by an incubation at 85 °C for 5 minutes to inactivate the enzyme.

For each RNA sample, a parallel no-RT control was prepared containing identical reaction components except the reverse transcriptase enzyme which was replaced by RNase-free water.

This control was run alongside experimental samples in downstream PCR to validate the absence of residual genomic DNA contamination.

Downstream PCR amplification of the synthesized cDNA was carried out EmeraldAmp® GT PCR Master Mix (2X). Each reaction utilized 0.5 µL of cDNA template. For the Shortissimo samples, amplification was performed using primers SwrA-YFP_fwd and eGFP n, yielding an expected product length of 159 bp. For the PB5980 and STlich samples, amplification was performed using primers vzdF and eGFP n, yielding an expected product length of 700 bp.

For each strain, a no-RT negative control was included in the amplification run, which showed no bands, confirming the absence of genomic DNA contamination.

4.0 Results and Discussion

4.1 γ-PGA Production Was Temperature Dependent

Previous work conducted in our laboratory, as well as other researchers [46], demonstrated that substantial γ-PGA is only produced at high temperatures, generally around 37 °C and up to 42 °C. This phenotype can be readily observed by growing γ-PGA-producing strains on LB agar plates, where colonies exhibit a characteristic glossy, highly mucoid appearance due to the accumulation of extracellular γ-PGA. As shown in Figure 4.1, PB5390 strain (*degS200^{Hy}, swrA^{+})* produced abundant γ-PGA when grown at 37 °C. In contrast, when grown at 24 °C, γ-PGA production was severely impaired, and colonies closely resembled those of the non-producer PB5249 strain (wild type *degS*, *swrA*$^{+}$), which does not exhibit the mucoid phenotype under these conditions.

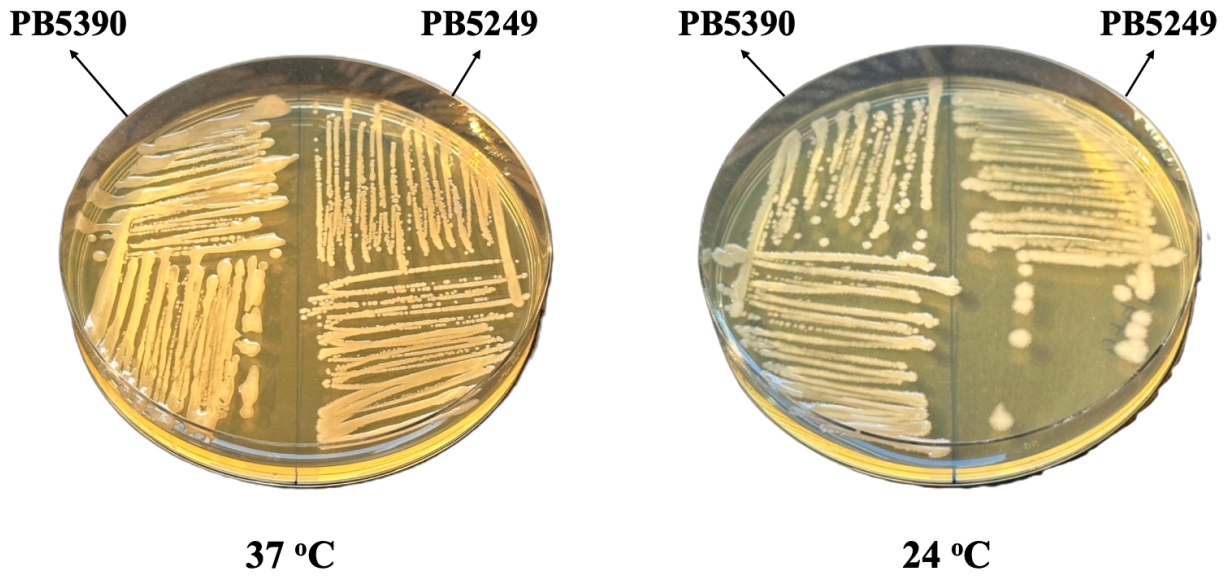

Figure 4.1. Temperature-dependent γ-PGA production on LB agar plates. PB5390 (*degS200^{Hy}, swrA^{+})* and PB5249 (*degS*, *swrA*$^{+}$) were incubated for 16 hours at 37 °C or 40 hours at 24 °C. Colonies producing γ-PGA exhibit a characteristic glossy, highly mucoid phenotype. The experiment was repeated three times, and the same phenotype was observed.

4.2 *pgsB* Expression Was Temperature Dependent

Given that γ-PGA production depends on the expression of the *pgs* operon [38], the reporter gene for the superfolder green fluorescent protein (*sfGFP*) inserted few nucleotides downstream of the ORF of the first gene of the operon, *pgsB*, preceded by a strong ribosome binding site (RBS) from the *spoVG* gene [25], was used for investigating the expression of *pgs* at different temperatures. The strain PB5745 carrying the *PpgsB-sfGFP* transcriptional reporter construct in a *degS200^{Hy}, swrA^{+}* background, was grown in LB broth at 24 °C and 37 °C, and samples were collected two hours after the transition point (T_2) (Figure 4.2) to record fluorescence emission as well as the optical densities with a microplate reader. The T_2 time point was selected based on previous work demonstrating detectable *PpgsB-sfGFP* reporter activity at this stage of growth [25].

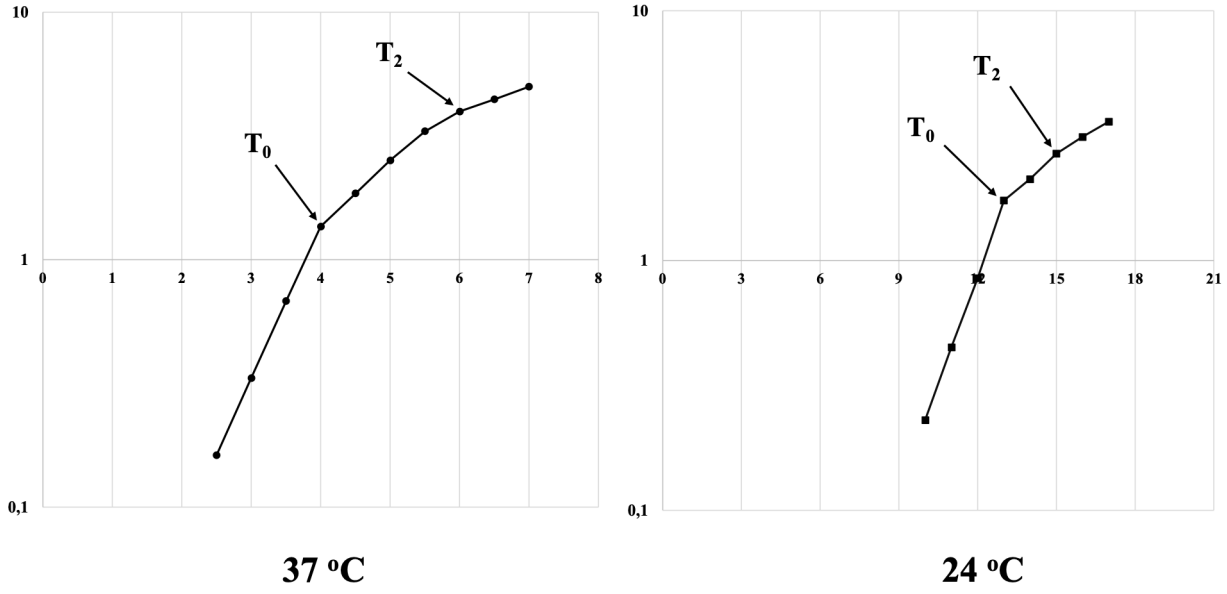

Figure 4.2. Representative growth curves and sampling time points at 37 °C (left) and 24 °C (right). Growth was started from spores inoculated in LB broth and optical density (OD_{600}) was monitored over time (time in hours on the X-axis, OD_{600nm} in logarithmic scale on the Y-axis) to identify key physiological growth phases across tested strains. Arrows indicate the transition point from exponential to stationary phase (T_0) and two hours after the transition phase (T_2), the time point selected for fluorescence intensity readings.

As shown in Figure 4.3, the average relative fluorescence intensity normalized to OD_{600} for *pgs* was above 40,000 at 37 °C, whereas it reached only approximately 1,500 at 24 °C. This represents a more than 25-fold difference in *pgsB* promoter activity between the two temperatures, indicating that low temperatures strongly reduced *pgsB* expression.

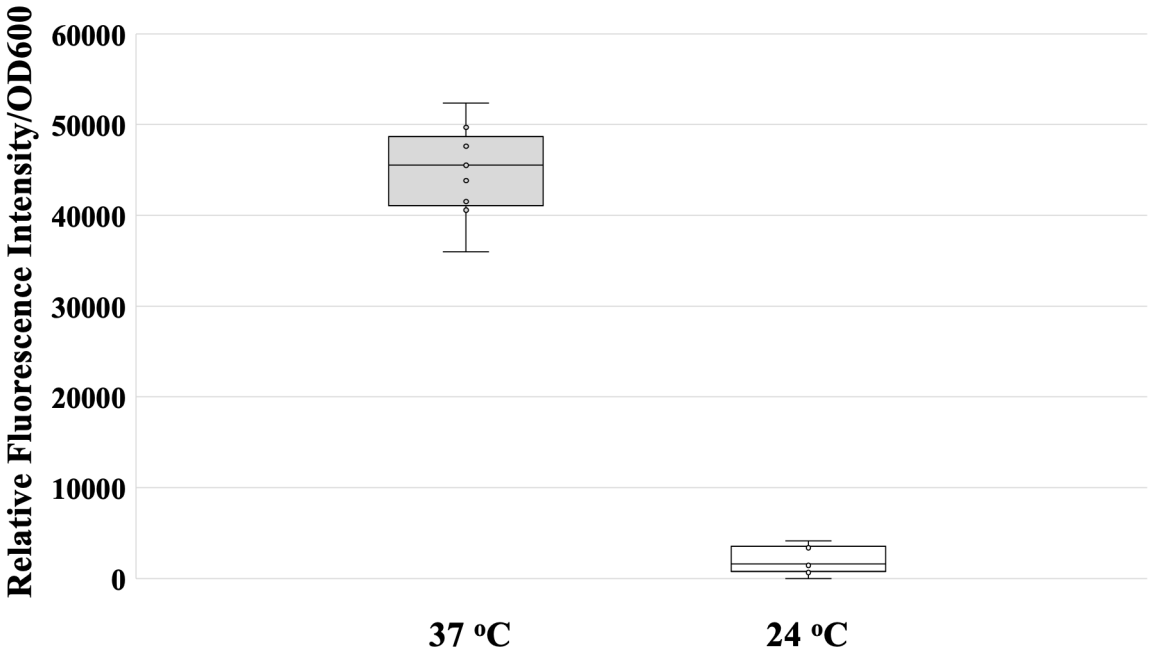

Figure 4.3 Temperature-dependent *pgsB* expression. PB5745 (*degS200^{Hy}, swrA^{+}, P_{pgsB}-sfGFP*) was grown in shaking flasks at 37 °C (left) and 24 °C (right), and samples were collected at T_2. Fluorescence intensity was background-subtracted using the auto-fluorescence signal obtained from the non-fluorescent negative control strain PB5390 and then normalized to OD_{600}. The experiments were repeated three times, and the mean and distribution of the individual measurements were plotted using Microsoft Excel.

4.3 A Potential RNA Thermometer Structure Was Predicted in the mRNA of *swrA*

Since functional SwrA is required for *pgsB* expression [31], we investigated whether *swrA* expression was regulated by temperature. First, *swrA* mRNA secondary structures were predicted using the ViennaRNAfold server (http://rna.tbi.univie.ac.at/), which identified a potential RNA structure that could mask the ribosome-binding site at lower temperatures.

As shown in Figure 4.4, the predicted base-pairing between the “CCC” sequence and the complementary “GGGGG” may sequester the RBS at lower temperatures and thereby inhibit translation. To disrupt this predicted interaction, site-directed mutagenesis was performed to replace the “CCC” sequence with “TTT”. According to the predicted RNA folding model, this

mutation should disrupt formation of the translation-inhibitory structure at lower temperatures. To test this hypothesis, the wild-type 5'UTR of *swrA* was replaced with the mutant form, and γ-PGA production from the wild type (WT) and mutant (MUT) SwrA strains was compared at 37 °C and 24 °C.

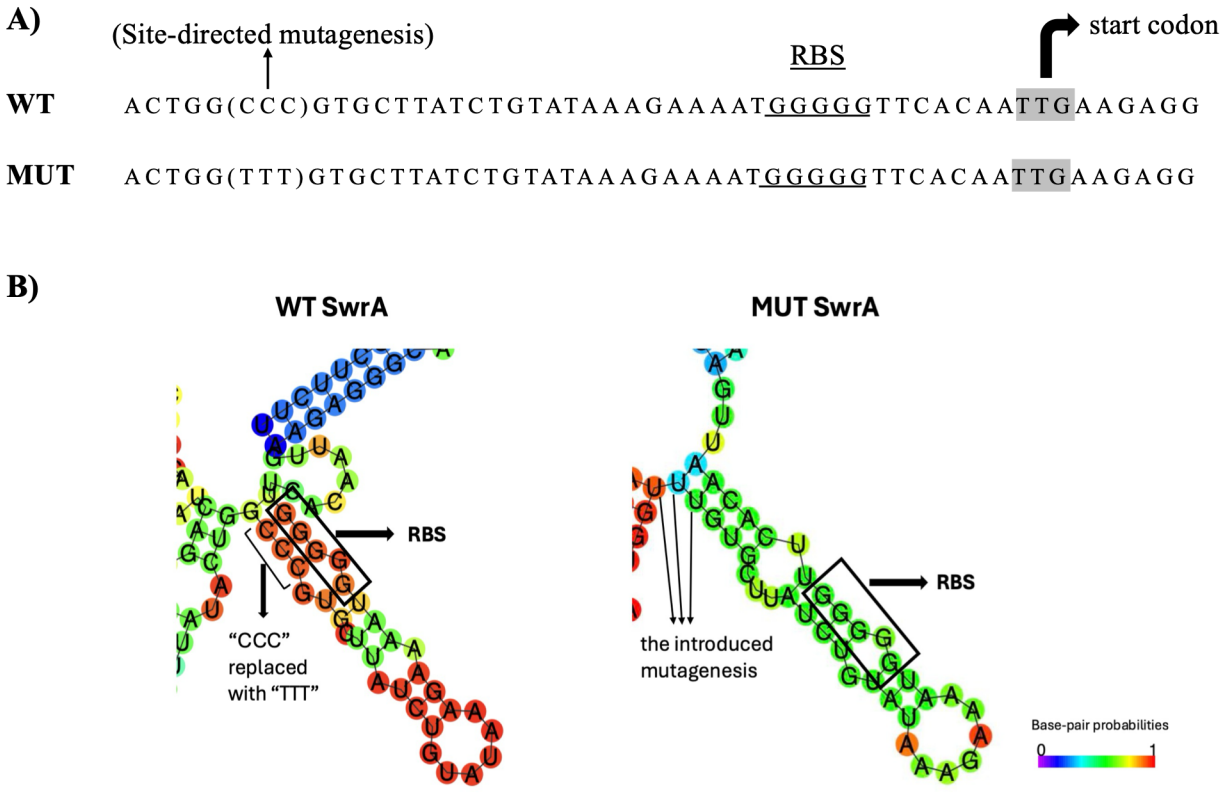

Figure 4.4. Predicted mRNA secondary structures of WT and MUT 5'UTR of *swrA*. (A) Sequence alignment showing the CCC to TTT substitution upstream of the ribosome binding site (RBS; GGGGG) and TTG start codon. (B) Disruption of the base-paired stem in MUT swrA, resulting in a less rigid, single-stranded conformation around the RBS compared to WT. Predictions were made by ViennaRNAfold server.

LB agar plates were incubated for 16 hours at 37 °C and 40 hours at 24 °C to assess the level of γ-PGA production. No significant difference in γ-PGA production was observed between the PB5974 (*degS200*^{Hy}, WT-5'UTR *swrA*) and PB5975 (*degS200*^{Hy}, MUT-5'UTR *swrA*) strains at either 37 °C or 24 °C (Figure 4.5). These results suggest that the predicted RNA thermometer structure in the *swrA* mRNA is unlikely to form and be responsible for the temperature-dependent

regulation of γ-PGA production. However, the expression of *swrA* at different temperatures was still unknown.

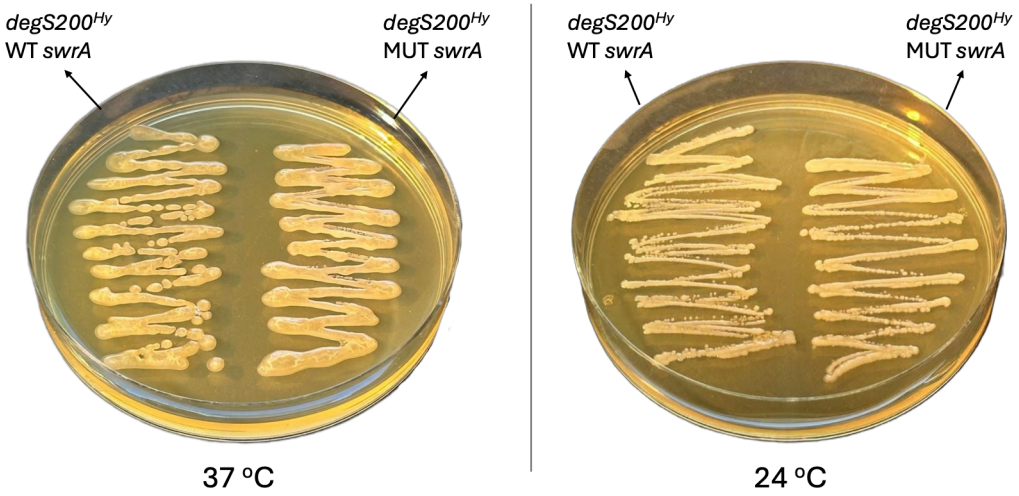

Figure 4. 5. γ-PGA production on LB agar plates. PB5974 (*degS200*^{Hy}, WT-5'UTR *swrA*) and PB5975 (*degS200*^{Hy}, MUT-5'UTR *swrA*)) strains were incubated for 16 hours at 37 °C or 40 hours at 24 °C. The experiment was repeated three times, and the same phenotype was observed.

4.4 SwrA-YFP Fusion Was Functional

To investigate whether *swrA* expression levels differ at 24 °C and 37 °C, the yellow fluorescent protein (YFP) was cloned to 3'end of the last amino acid of SwrA, creating a chimeric protein. The fusion of YFP to SwrA could potentially interfere with the activity of both proteins; therefore, the functionality of the chimera needed to be evaluated before use.

The construct was inserted into the PB5470 (Δ*swrA*) at the ectopic *pks* locus and fluorescence emission was verified with TECAN microplate reader. Then, since SwrA is required for swarming motility [27,28], the functionality of the *swrA* gene in the chimeric protein was tested by determining whether it could restore the swarming defect of a Δ*swrA* strain.

The recipient strain PB5470 (Δ*swrA*) was used as the negative control, whereas PB5249 (*swrA*+) was used as the positive control. Introduction of the SwrA-YFP fusion construct into PB5470 restored the swarming phenotype (Figure 4.6), demonstrating that the fusion protein retained SwrA activity.

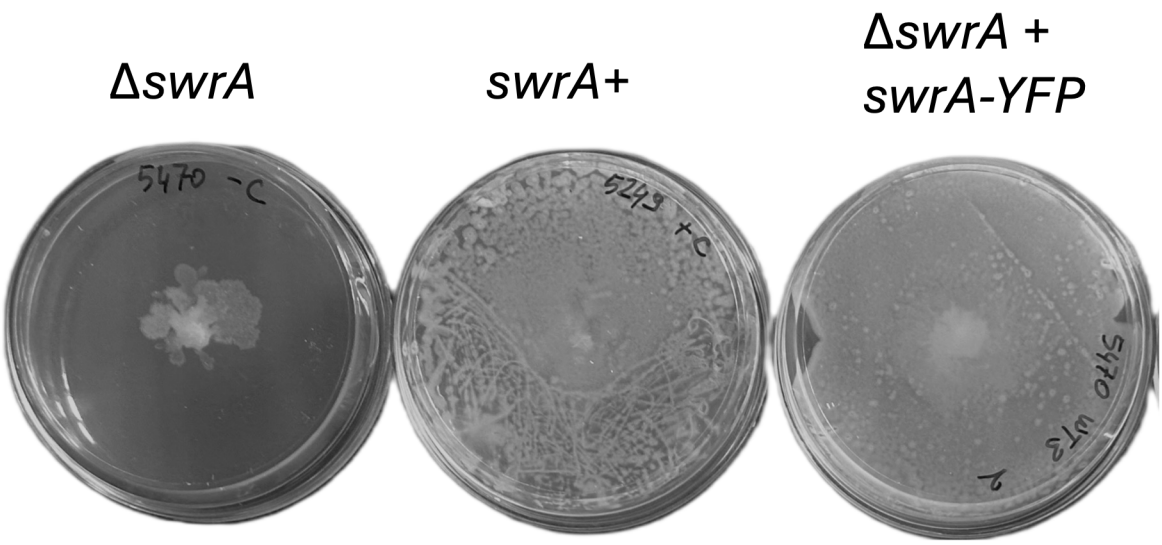

Figure 4.6. Swarming assay on LB+0.7% Agar. Plates were incubated overnight at 30 °C.

4.5 *swrA* Expression Is Not Reduced at 24 °C

Following confirmation that the SwrA-YFP fusion is functional, the construct was used to investigate *swrA* expression at 24 °C and 37 °C. As already described, *swrA* gene has two promoters and the sig^D-dependent one is the sole working in liquid growth in the absence of DegU-P [26]. To determine whether disrupting the predicted 5′UTR secondary structure and exposing the RBS affected sig^D-dependent *swrA* expression, the 5′UTR mutation described in Figure 4.4 was introduced upstream of the chimeric SwrA-YFP reporter. The resulting constructs, with and without the mutation, were transformed into the PB5470 (Δ*swrA*) genetic background to eliminate any contribution from endogenous *swrA*, in the absence of the $degS200^{Hy}$ mutation.

Liquid growth both at 24 ° C and 37 °C was followed by OD_{600} reading to collect samples at T_2, and fluorescence intensity was measured at both temperatures. Surprisingly, *swrA* expression from the native 5'UTR was higher at 24 °C than at 37 °C. Moreover, at both temperatures, the presence of the 5' UTR mutation reduced *swrA* expression compared to the wild-type (Figure 4.7). At 24 °C, the expression of the WT *swrA* was 1.4-fold higher than that of the MUT *swrA* allele, while at 37 °C, WT *swrA* expression was 2.2-fold higher than MUT *swrA* expression. These findings suggest that sig^D-dependent *swr*A expression is not reduced at low temperatures and that the predicted RNA secondary structure identified in silico does not play the expected thermometer role on the P_{sigD} mRNA. Rather, the introduced mutation may have impaired *swrA* transcription or translation.

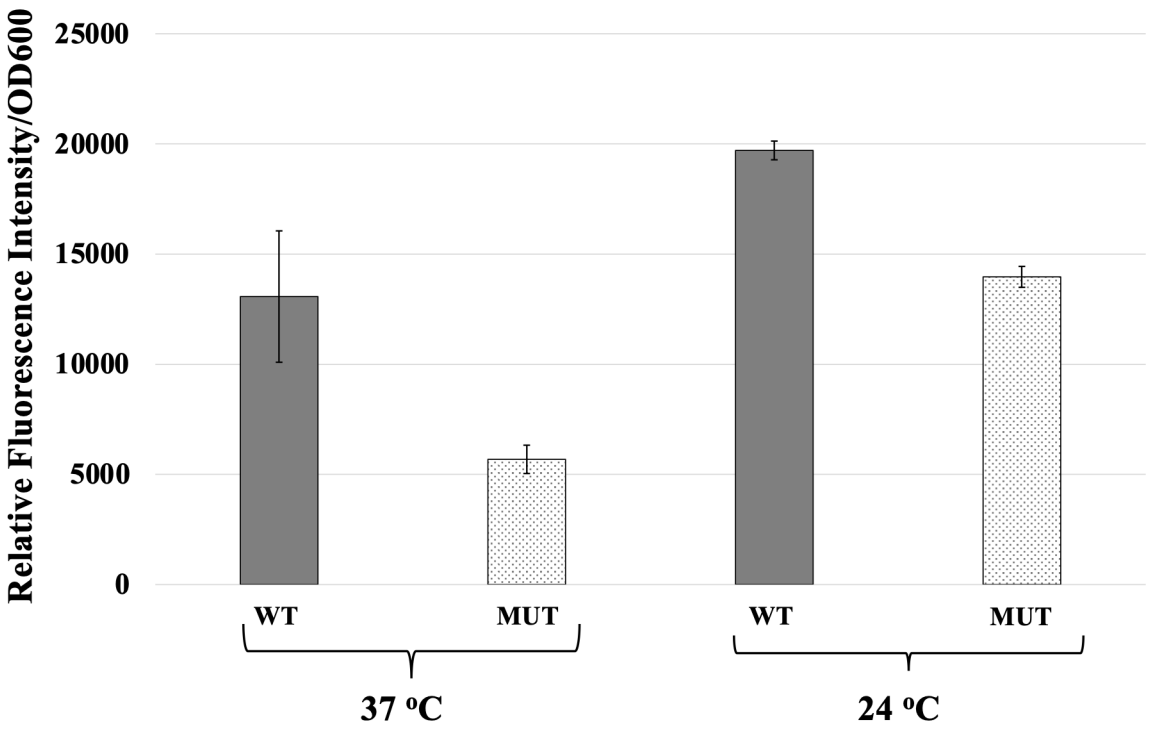

Figure 4.7. sig^{D}-dependent *swrA* expression in liquid. PB5980 (Δ*swrA,* WT-5'UTR *swrA-yfp*) and PB5981 (Δ*swrA,* MUT-5'UTR *swrA-yfp*) were grown in LB broth at 24 °C and 37 °C, and samples were collected at T_2. Fluorescence intensity was background-subtracted using the auto-fluorescence signal obtained from the non-fluorescent negative control strain PB5249 and then normalized to OD_{600}. The experiments were repeated three times, and data represent the mean of three independent experiments, and error bars indicate the standard deviation.

To measure sig^{A}-dependent *swrA* expression and verify the effect of the 5'UTR mutation on the sig^{A}-dependent transcript, both the wild-type and mutant SwrA-YFP fusion constructs were introduced into PB5390 (*degS200Hy, swrA*$^{+}$), the genetic asset necessary for the γ-PGA production.

Strains were grown in liquid culture at both temperatures until T_2, after which fluorescence intensity was measured. As shown in Figure 4.8, YFP fluorescence was detected at both 24 °C and 37 °C. Importantly, *swrA* expression was similar at the two temperatures, with average fluorescence intensities normalized to OD_{600} of approximately 4,600 at 24 °C and 4,800 at 37 °C. The wild-type construct, again, showed higher expression levels than the mutant construct at both temperatures. At 24 °C, WT *swrA* expression was 1.7-fold higher than that of the mutant allele, whereas at 37 °C, it was 1.2-fold higher.

The sig^A-dependent expression from the wild-type constructs inserted in the *degS200^{Hy}* background was lower compared with the sig^D-dependent expression at both temperatures, corresponding to approximately 24% at 24 °C and 35% at 37 °C.

Together, these findings demonstrate that *swrA* expression is not reduced at 24 °C under either the sig^A- or sig^D-dependent regulation. Notably, in the *degS200^{Hy}* background, *swrA* expression was readily detected at T_2 during growth at 24 °C, whereas *pgsB* expression was nearly undetectable under the same conditions (Fig. 4.3). Therefore, the temperature-dependent decrease in *pgsB* expression and γ-PGA production cannot be explained by reduced *swrA* expression. Moreover, disruption of the predicted 5′ UTR secondary structure did not increase *swrA* expression as expected for either the sig^A- or sig^D-dependent transcripts, confirming that this structure does not function as the predicted translation-inhibitory RNA thermometer.

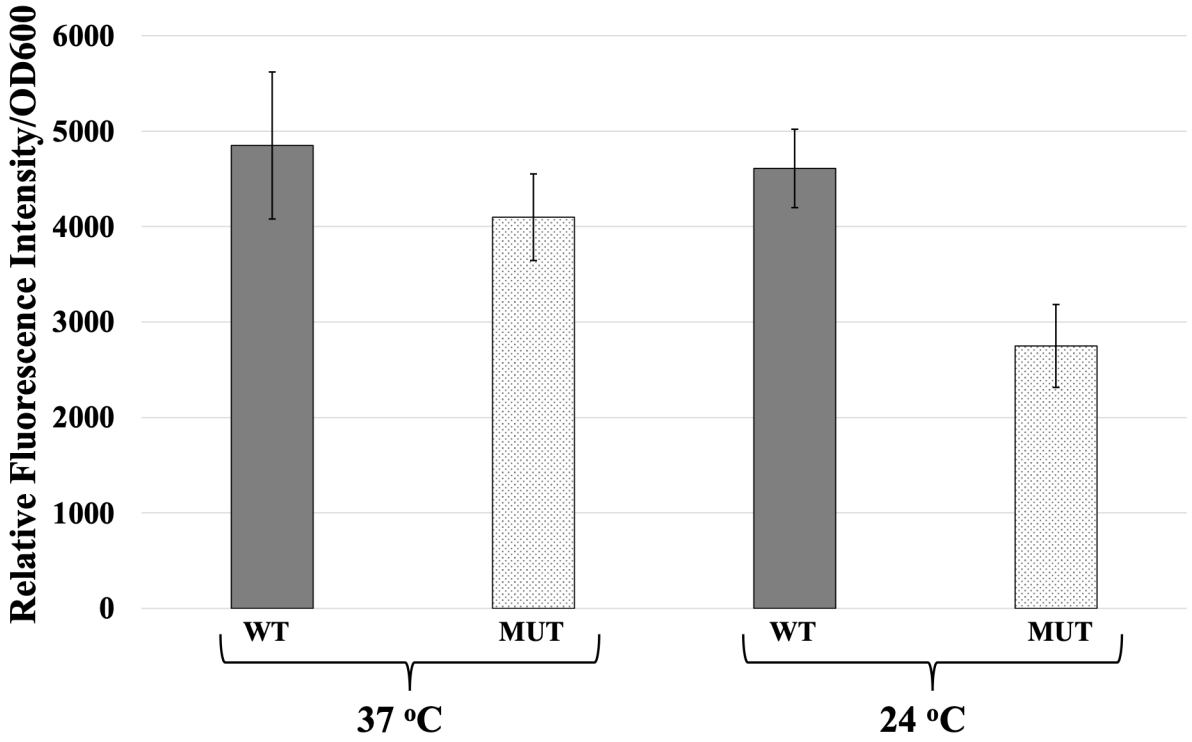

Figure 4.8. sig^A-dependent *swrA* expression during liquid growth. PB5978 (*degS200^{Hy},* WT-5'UTR *swrA-yfp*) and PB5979 (*degS200^{Hy},* MUT-5'UTR *swrA-yfp)* were grown in LB broth at 37 °C (left) and 24 °C (right), and samples were collected at T_2. Fluorescence intensity was background-subtracted using the auto-fluorescence signal obtained from the non-fluorescent negative control strain PB5390 and then normalized to OD_{600}. The experiments were repeated three times, and data represent the mean of three independent experiments, and error bars indicate the standard deviation.

4.6 Overexpression of SwrA Did Not Restore γ-PGA Production at 24 °C

To definitely prove that SwrA is not responsible for the cold-phenotype of P_{pgsB}, we investigated whether increasing the levels of SwrA could overcome the low γ-PGA production observed at 24 °C. A plasmid carrying *swrA* under the control of the IPTG-inducible $P_{hyper\text{-}spank}$ promoter was introduced into PB5390 (*degS200*^{Hy}*, swrA*$^{+}$*)*. The resulting strain was induced with 0.5 mM IPTG to overexpress *swrA* and polymer production was analyzed on LB agar plates following incubation for 16 hours at 37 °C or 40 hours at 24 °C.

Strikingly, overexpression of *swrA* failed to restore γ-PGA production at 24 °C (Figure 4.9). This result indicates that increasing the cellular level of SwrA is not sufficient to overcome the temperature-dependent reduction in γ-PGA production. Thus, even when SwrA is present at elevated levels, *pgs* expression remains strongly reduced at 24 °C, suggesting that another component required for *pgs* activation may limit the polymer biosynthesis under these conditions.

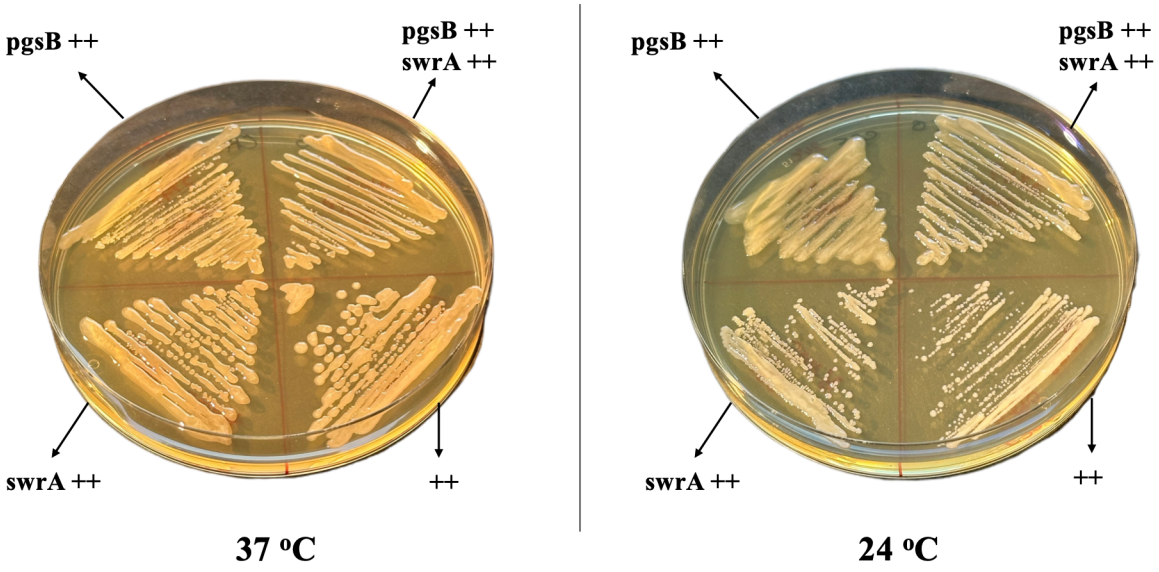

Figure 4.9. Overexpression of *swrA* failed to restore γ-PGA production at 24 °C.

LB agar plates with chloramphenicol and 0.5 mM IPTG were incubated for 16 hours at 37 °C or 40 hours at 24 °C. γ-PGA synthesis is indicated by a mucoid colony phenotype. At 37 °C, all strains displayed a mucoid phenotype, including the negative control carrying the empty vector. At 24 °C, mucoid phenotype was observed only upon overexpression of *pgsB* (*pgsB* ++ and *pgsB* ++ *swrA* ++), whereas overexpression of *swrA* alone (*swrA* ++) or the empty vector control (++) failed to restore γ-PGA production. "++" indicates gene overexpression driven by the $P_{hyper\text{-}spank}$ promoter, while the standalone "++" label denotes the negative control strain carrying the empty $P_{hyper\text{-}spank}$ vector.

Together with the SwrA-YFP expression data presented previously, these findings confirm that impaired γ-PGA production at 24 °C is not caused by reduced SwrA levels.

To verify whether cells grown at 24 °C retained the capacity to synthesize γ-PGA, *pgsB* was overexpressed as a positive control, which successfully restored γ-PGA production. Given that full activation of the *pgs* operon depends on cooperative regulation by both SwrA and DegU-P [31], our focus shifted to investigating the role of DegU-P in the temperature-dependent regulation of *pgs* expression.

4.7 *aprE* Expression Was Temperature Dependent

The previous results indicated that the reduced *pgsB* expression observed at 24 °C was not associated with a reduced *swrA* expression. Since both SwrA and DegU-P are required for efficient *pgs* expression [31], we next investigated whether reduced DegU-P activity could explain the lower *pgsB* expression at 24 °C.

To examine this possibility, the expression of *aprE*, a well-established DegU-P target gene, which is negatively regulated by SwrA, was examined at 24 °C and 37 °C. Two strains containing a P_{aprE}-*gfp* reporter construct and only differing for the presence or absence of a functional *swrA* gene [25] were used. PB5723 (*degS200*^{Hy}, *swrA*$^{+}$, P_{aprE}-*gfp*) and PB5725 (*degS200*^{Hy}, Δ*swrA*, P_{aprE}-*gfp*) strains were grown at 24 °C and 37 °C untill T_2 and fluorescence intensity was measured for both temperatures.

As shown in Figure 4.9, in the absence of *swrA*, P_{aprE}-*gfp* expression was more than 10-fold higher at 37 °C than at 24 °C. Since activation of the *aprE* promoter is dependent on DegU-P alone, these results indicate that DegU-P activity is significantly lower at 24 °C than at 37 °C. In the presence of *swrA* allele, P_{aprE}-*gfp* expression was reduced at both temperatures compared with the Δ*swrA* background. This is consistent with SwrA being present at both temperatures and negatively affecting P_{aprE} promoter activation [25].

Taken together, these results suggest that, rather than a lack of *swrA*, a reduced DegU-P activity is likely the cause of the lower *pgs* expression and γ-PGA production at 24 °C. The regulation of DegU-P is particularly complex because its cellular activity depends not only on phosphorylation by DegS but also on the stability of the phosphorylated protein. Several mechanisms could therefore account for the reduced DegU-P activity. First, growth at low temperatures may directly diminish the enzymatic rates of the sensor kinase DegS, decreasing the frequency of

autophosphorylation or subsequent phosphotransfer to DegU; this could reflect a general reduction in kinase turnover at low temperature. Second, despite active phosphotransfer, steady-state intracellular levels of DegU-P may be limited by enhanced proteolytic degradation mediated by the ClpCP complex, which selectively targets DegU-P [53]. Third, DegU-P positively autoregulates *degU* transcription [19]; a failure to reach the critical threshold of DegU-P needed to sustain this feedback loop could keep total cellular DegU levels low. These regulatory mechanisms provide several possible ways through which temperature-dependent changes could alter the cellular levels of active DegU-P and consequently affect downstream gene regulation. To investigate these proposed mechanisms and evaluate the expression profiles of these key regulatory components across temperatures, we investigated the transcriptome-wide probing dataset established by Jolley et al. [50], as detailed in the following chapter.

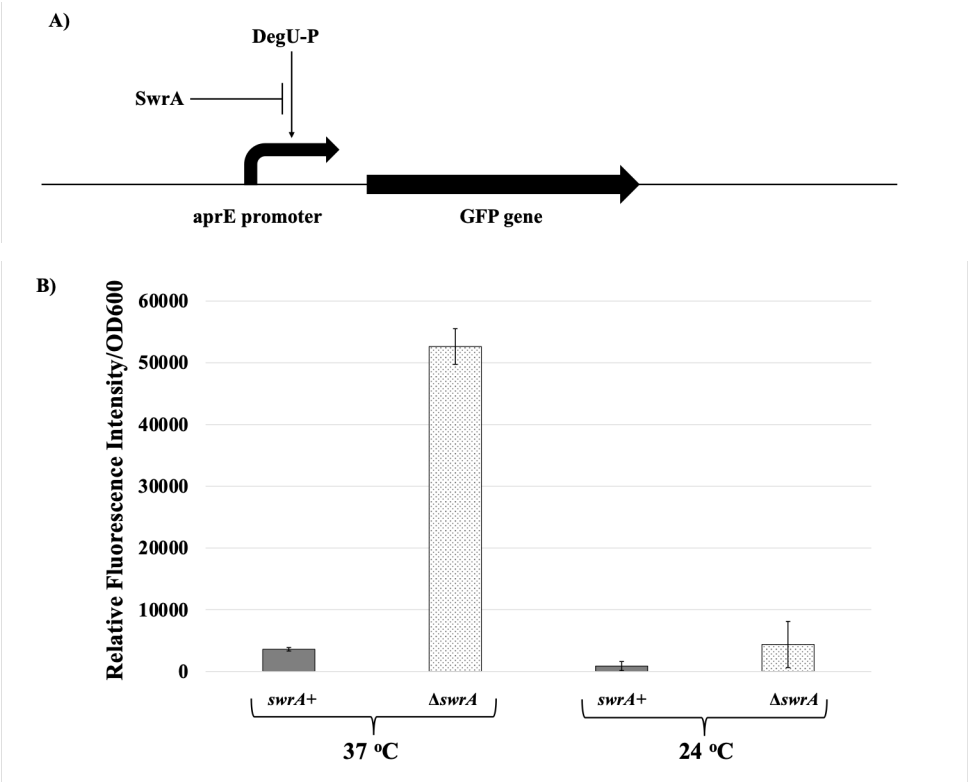

Figure 4.9. Temperature-dependent *aprE* expression.

(A) Schematic representation of P_{aprE} activation. (B) PB5723 (*degS200*^{Hy}*, swrA*$^{+}$*,* P_{aprE}*-gfp*) and PB5725 (*degS200*^{Hy}*,* Δ*swrA,* P_{aprE}*-gfp*) strains were grown in LB broth at 37 °C (left) and 24 °C (right), and samples were collected at T_2. Fluorescence intensity was background-subtracted using the auto-fluorescence signal obtained from the non-fluorescent negative control strain PB5390 and then normalized to OD_{600}**.** The experiments were repeated three times, and data represent the mean of three independent experiments, and error bars indicate the standard deviation.

4.8 Transcriptome-Wide Analysis Reveals Reduced *degU* Expression at Low Temperature

The transcriptome-wide gene expression data analyzed were obtained from the RNA thermometer probing dataset generated by Jolley et al. [50]. The processed transcript abundance data, reported as transcripts per million (TPM), were used to examine the expression of selected genes involved in the DegS-DegU regulatory pathway at different growth temperatures. The dataset was generated using a *B. subtilis* strain PLBS338 carrying a wild-type *degS* allele and lacking functional *swrA* (*swrA*$^{-}$), whereas the experiments presented in this thesis to investigate γ-PGA production were mainly conducted in a *degS200*^{Hy}*, swrA*$^{+}$ background. Although the genetic backgrounds differ, the dataset was used to examine general temperature-dependent changes in the transcription of selected regulatory genes. Transcript abundance was compared between cells grown at 23 °C and 37 °C for selected genes.

Analysis of the transcriptome-wide dataset revealed that *degU* transcript abundance was approximately 2.4-fold higher at 37 °C than at 23 °C, whereas *degS* transcript abundance remained relatively unchanged between the two temperatures. Since the *degSU* operon is controlled by three promoters, including P3, which is located between *degS* and *degU* and activated by DegU-P [19], the reduced *degU* transcript abundance at 23 °C may indicate that DegU-P activity does not reach the threshold required to sustain P3-dependent positive autoregulation. Failure to sustain this positive-feedback loop could subsequently reduce the cellular abundance of DegU, further limiting the amount of DegU available for phosphorylation and thereby reinforcing the reduction in DegU-P activity.

The dataset also revealed temperature-dependent changes in genes associated with the ClpCP proteolytic system. MecA acts as an adaptor protein that targets specific substrates to the ClpCP protease, thereby promoting their proteolytic degradation [53]. Abundance of *mecA* transcript was approximately 2.1-fold lower at 37 °C than at 23 °C, whereas *clpC* and *clpP* transcript abundance was approximately 1.7- and 2.1-fold higher at 37 °C, respectively. The higher *mecA* expression at 23 °C could therefore be consistent with increased MecA-mediated targeting of substrates for proteolysis at low temperature. However, the opposing temperature-dependent expression patterns of *mecA* and the *clpCP* components make it difficult to predict how the overall capacity of the proteolytic system might be affected by temperature. Moreover, transcript abundance does not directly reflect the activity of the ClpCP protease or the rate of substrate degradation. Therefore, these data do not establish whether altered ClpCP-mediated proteolysis of DegU-P contributes to

the reduced DegU-P activity observed at low temperature. Nevertheless, the temperature-dependent changes in the expression of these components provide a possible regulatory link that warrants further investigation.

Analysis of selected DegU-regulated genes revealed distinct temperature-dependent expression patterns. Transcript abundance of *pgsB* was approximately 1.5-fold higher at 37 °C than at 23 °C. This difference should be interpreted cautiously because the dataset was generated in a *swrA*⁻, *degSU* wild-type background. In the absence of SwrA, *pgsB* cannot be activated by DegU-P [31]. Moreover, the *swrA* locus is prone to frameshift mutations, and a fraction of cells in the analyzed population has likely acquired a functional *swrA* allele, potentially contributing to the low level of *pgsB* transcription detected. This is consistent with previous observations showing that a wild-type *degSU* background does not produce detectable levels of γ-PGA even in the presence of functional *swrA*, whereas the $degS200^{Hy}$ or $degU32^{Hy}$ mutation, which enhances DegU-P activity, is required for detectable γ-PGA production [25,31]

Similarly, *aprE* transcript abundance was only approximately 1.1-fold higher at 37 °C than at 23 °C. However, *aprE* expression is strongly dependent on DegU-P activity, and robust expression of DegU-P-dependent degradative enzymes is typically observed in backgrounds with enhanced DegU-P activity, such as $degS200^{Hy}$ or $degU32^{Hy}$ strains [25]. Since the dataset was obtained in a wild-type *degSU* genetic background, the very low *aprE* transcript abundance at both temperatures limits the significance of this small difference.

In contrast, the abundance of the *flgB* transcript, the first gene of the *fla/che* operon, showed a pronounced temperature-dependent difference, being approximately 6.7-fold higher at 23 °C than at 37 °C. Unlike *aprE* and *pgsB*, whose efficient activation requires high levels of DegU-P as those produced by Hy mutations, in a wild-type *degSU* genetic background, the normal level of DegU-P is sufficient to have an impact on *fla/che* operon expression [24,26]. The outcome of the DegU-P impact of *fla/che* depends on the presence of SwrA. In the absence of SwrA, DegU-P promotes repression, whereas in its presence, SwrA promotes DegU-P-dependent activation of these genes [24,25]. Therefore, the substantially higher *flgB* transcription at 23 °C in the $swrA^{-}$ dataset suggests that DegU-P-dependent repression of the *fla/che* operon is reduced at 23 °C compared with 37 °C or that DegU is not yet phosphorylated at the time of sampling (at mid-log phase). At any rate, the temperature-dependent derepression of *fla/che* would be consistent with a reduced DegU-P activity observed at low temperature, as evidence in our data (Fig. 4.9).

Table 4.1. Temperature-dependent transcripts per million (TPM) abundance of selected genes involved in DegU regulation and its downstream pathways [50].

Gene Name	**Locus Tag**	**Pathway Role**	**23°C (TPM)**	**37°C (TPM)**	**Shift in Cold**
degU	BSU35490	Master Response Regulator	198.59	467.55	Decline (~2.4-fold decrease)
degS	BSU35500	Sensor Histidine Kinase	172.11	156.13	Stable
mecA	BSU11520	Target-Specific Adaptor	253.47	121.77	Surge (~2.1-fold increase)
clpC	BSU00860	AAA+ Chaperone Subunit	168.38	289.28	Decline (~1.7-fold decrease)
clpP	BSU34540	Core Proteolytic Peptidase	24,973.87	51,210.12	Decline (~2.1-fold decrease)
flgB	BSU16180	Flagellar Basal Body	216.57	32.29	Surge (~6.7-fold increase)
pgsB	BSU35900	Poly-γ-glutamic Acid Synthesis	5.25	8.12	Decline (~1.5-fold decrease)
aprE	BSU10300	Alkaline Exoprotease	0.82	0.93	Decline (~1.1-fold decrease)

4.9 Spontaneous Frameshift Mutations in *swrA* Caused Phenotypic Heterogeneity

One of the major challenges encountered during our experiments was the high variability in the *swrA* expression levels between replicates, which was attributed to spontaneous frameshift mutations in *swrA*. As discussed in the Introduction, the *swrA* gene contains a homopolymeric A-tract that is prone to insertion and deletion mutations, which results in frameshifts and loss of functional SwrA. The frameshifting mutation in *swrA* may represent a fitness advantage for bacterial cells, by abolishing energy consuming pathways such as flagella and γ-PGA production, which are not essential under laboratory growth conditions, allowing $swrA^-$ to become enriched in the population. In fact, domesticated laboratory strains, such as *B. subtilis* 168 and PY79, commonly carry a non-functional frameshifted *swrA* allele ($swrA^-$) [27].

Unfortunately, frameshifts in *swrA* would affect both on the P_{swrA}-reporter system and on the P_{pgsB}-reporter: 1) as the YFP reporter coding sequence was fused to the *swrA* ORF, a frameshift in the *swrA* ORF would cause a frameshift in the YFP coding region, with loss of fluorescence emission; 2) P_{pgsB} is only expressed in $swrA^+$ cells (Figure 4.10), and if $swrA^-$ cells take over in the cultures, the global GFP fluorescence in the sample would decrease.

When the work begun, growth assays were started from an overnight-grown (O/N) pre-inoculum. This procedure extended the total incubation time, providing more opportunity for spontaneous frameshift mutations in *swrA* to arise and become enriched in the population.

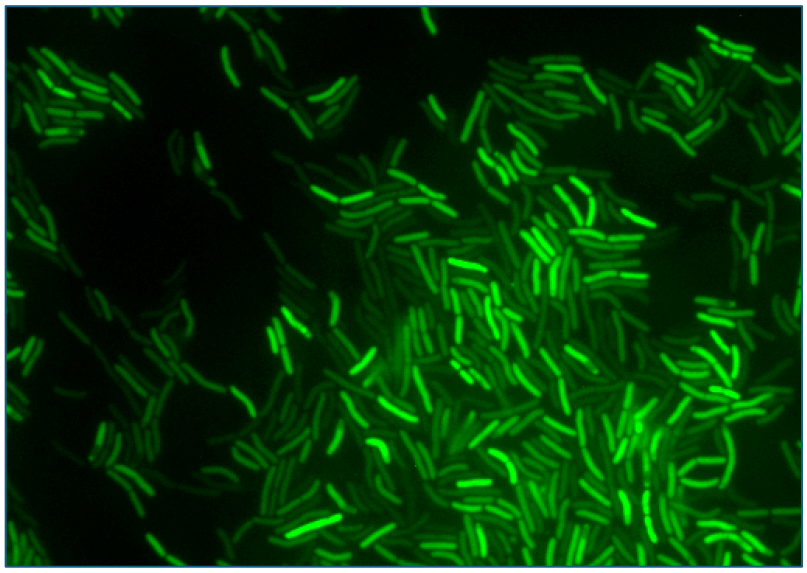

Figure 4.10. Fluorescence microscopy of PB5745 ($degS200^{Hy}$, $swrA^+$, P_{pgsB}-*sfGFP*) showing cell-to-cell variability in fluorescence levels.

To overcome this limitation, in the subsequent work, growth curves were initiated directly from spores. Spores were first resuspended in a small volume of LB broth and then equally distributed into the larger volumes of LB broth used for each replicate. To compare the variability between two methods, six biological replicates of strain PB5745 (*degS200^{Hy}, swrA^{+}, P_{pgsB}-sfGFP*) were grown at 24 °C and 37 °C, and samples were collected at T_2 for GFP fluorescence measurements. Compared with cultures initiated from O/N growth, the spore-based method doubled the mean fluorescence from approximately 20,000 to 40,000 while substantially reducing variability between replicates. The coefficient of variation decreased from approximately 62.5% for overnight cultures to 15% for spore-derived cultures, indicating markedly improved reproducibility (Figure 4.11). All growth assays and fluorescence measurements presented in this thesis were performed using this spore-based method.

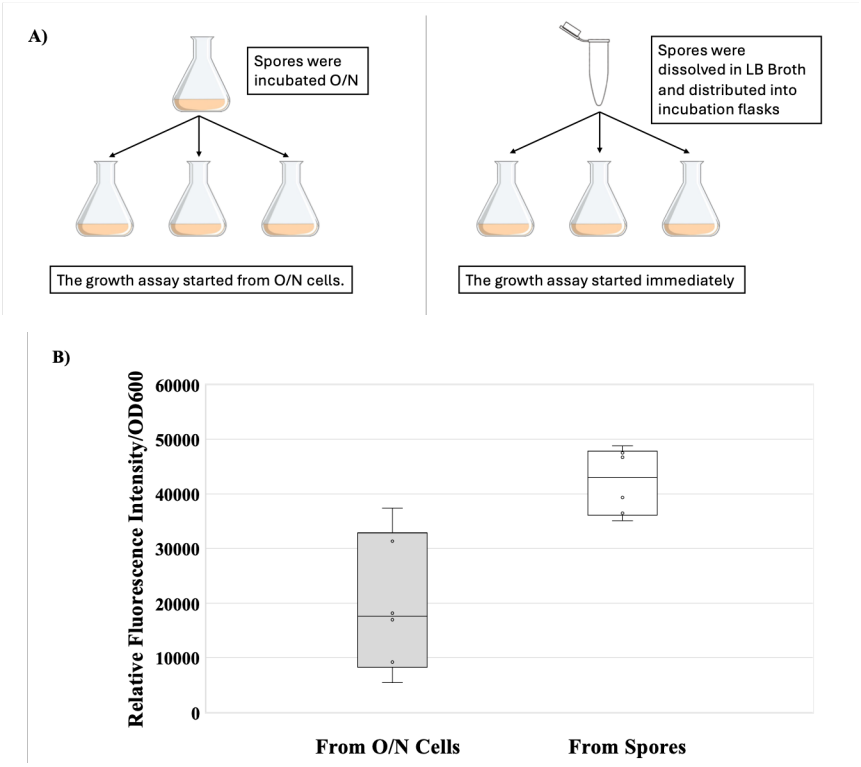

Figure 4.11. Comparison of P_{pgsB} fluorescence emission at 37 °C from several replicates grown according the two experimental protocols. (A) Schematic representation of the two experimental protocols used for comparison. (B) PB5745 (*degS200^{Hy}, swrA^{+}, P_{pgsB}-sfGFP*) was grown in LB broth at 37 °C, and samples were collected at T_2. Fluorescence intensity was background-subtracted using the auto-fluorescence signal obtained from the non-fluorescent negative control strain PB5390 and then normalized to OD_{600}. The experiment was performed with six biological replicates, and the mean and distribution of the individual measurements were plotted using Microsoft Excel.

4.10 Development of Stable *swrA* Constructs

We decided to develop new *swrA* constructs to investigate *swrA* expression by removing the homopolymeric A-tract, thereby preventing spontaneous frameshift mutations and the resulting variation in experimental results.

The first strategy was the insertion of the YFP gene directly downstream of the *swrA* promoter, creating the P_{swrA}-*yfp* construct. However, this construct produced no detectable fluorescence above the negative control. The absence of fluorescence signal could have resulted either from insufficient transcription of the construct or from a lack of translation.

Following the failure of the first construct to produce detectable YFP fluorescence, a second strategy was used to investigate *swrA* expression. In the second construct, the first 7 amino acids of SwrA ($SwrA_{1-7}$) were fused in frame with YFP, creating the construct the P_{swrA}- $swrA_{1-7}$-*yfp*, referred to as "Shortissimo". The aim of this strategy was to facilitate YFP expression by retaining part of the native *swrA* sequence possibly required for efficient translation, while avoiding the homopolymeric A-tract, Surprisingly, the Shortissimo construct also produced no detectable fluorescence above the negative control.

The third strategy was inspired by nature. *B. licheniformis* also contains a gene encoding a SwrA protein that shares 85.5% identity and 93.2% similarity with *B. subtilis* SwrA [28]. The homopolymeric A-tract of *B. licheniformis swrA* gene contains six adenine (6A) residues, instead of the eight adenine (8A) residues present in *B. subtilis swrA*. When we examined *swrA* sequences in the NCBI database, all *B. licheniformis* entries contained a 6A tract. In contrast, *B. subtilis swrA* sequences contained either 8A ($swrA^+$) or 9A ($swrA^-$) tracts, with similar percentages, and a small number of entries containing a 7A tract ($swrA^-$). This observation suggests that the *B. licheniformis* version of the *swrA* gene may be less prone to frameshift mutations. Based on these observations, site-directed mutagenesis was used to reduce the homopolymeric A-tract in *swrA* from 8A to 6A, mimicking the *B. licheniformis swrA* sequence. YFP was then fused in frame at the 3'-end of the full-lenght *swrA* sequence. Importantly, this modification maintained the same amino acid sequence of SwrA, as the nucleotide changes did not alter the protein coding sequence. The new construct was referred to as "STLich" (STabilized as Licheniformis). The STLich construct produced fluorescence at a similar level to WT *swrA-yfp* (data not shown). Therefore, STLich provided a promising construct for studying *swrA* expression in future experiments.

The complete absence of fluorescence from the P_{swrA}-*yfp* and Shortissimo constructs was unexpected and prompted the question of what was preventing YFP expression. To determine whether the lack of fluorescence was due to a transcriptional defect, RNA was isolated from the strain carrying the Shortissimo construct and analyzed by RT-PCR. The corresponding short *swrA* mRNA could be detected, confirming that the construct was indeed transcribed (data not shown). Therefore, the absence of YFP fluorescence is likely associated with a defect at the translational step.

Our initial analysis of the *swrA* mRNA secondary structure suggested the presence of a potential RNA thermometer, in which the RBS may be sequestered within a hairpin structure at low temperatures, potentially limiting its accessibility to the ribosome and thereby affecting translation initiation (Fig.4.4). However, the results obtained with the Shortissimo construct suggested another mechanism of translational regulation that is independent from temperature. Sequences downstream of the first 21 nucleotides, which have been removed in Shortissimo, may fold in an RNA structure that prevents formation of an RBS-sequestering structure in the native *swrA* transcript and promote efficient translation of the downstream YFP. Further experiments are required to determine whether this regulatory mechanism exist and is involved in *swrA* expression regulation.

Table 4.2. Comparison of *swrA* constructs with different A-tract lengths and their effects on transcription and YFP fluorescence.

***swrA* Construct**	***swrA* coding region**	**Homopolymeric A-tract**	**mRNA**	**YFP Fluorescence**
P*$_{swrA}$*-yfp	0	Absent	Unknown	Absent
Shortissimo	21 nt	Absent	Present	Absent
STLich	351 nt	6A	Present	Present
Native	351 nt	8A	Present	Present

5.0 Conclusions

This study demonstrates that γ-PGA production and *pgsB* expression in *B. subtilis* are strongly temperature-dependent, with both being robust at 37 °C but nearly undetectable at 24 °C. Since activation of the *pgs* operon requires both the phosphorylated response regulator DegU (DegU-P) and the regulatory protein SwrA, the study first investigated whether temperature-dependent regulation of SwrA could account for the reduced *pgsB* expression at 24 °C.

A predicted secondary structure in the 5′ UTR of *swrA* suggested the presence of a potential RNA thermometer that could regulate SwrA translation in response to temperature. However, disrupting the predicted structure did not restore γ-PGA production at 24 °C. Indeed, the wild-type SwrA-YFP construct showed higher expression than the mutant construct at both 24 °C and 37 °C, indicating that the introduced mutation did not increase *swrA* expression as expected. Furthermore, expression of the wild-type SwrA-YFP construct remained comparable between 24 °C and 37 °C, indicating that *swrA* expression itself is not reduced at low temperature. Finally, overexpression of *swrA* from an inducible promoter was not sufficient to restore γ-PGA production at 24 °C, directly confirming that reduced *pgsB* activation at low temperature is not a consequence of limiting SwrA levels.

The attention therefore turned to DegU-P, as the second regulatory factor required for efficient *pgs* activation. To assess DegU-P activity, the promoter activity of *aprE*, a well-established DegU-P-dependent gene whose expression is negatively regulated by SwrA, was examined in a Δ*swrA* genetic background. P_{aprE}-*gfp* expression was strongly reduced at 24 °C compared with 37 °C, indicating that DegU-P activity is substantially lower at 24 °C. The reduced DegU-P activity thus provides a mechanistic explanation for the lower *pgsB* expression and γ-PGA production observed at this temperature.

Several mechanisms may account for the reduced DegU-P activity. Low temperatures may reduce the enzymatic activity of the sensor kinase DegS, thereby limiting DegU phosphorylation, while enhanced ClpCP-mediated proteolysis could reduce the intracellular stability of DegU-P. In addition, failure to reach the DegU-P threshold required to sustain positive autoregulation of *degU* could reduce cellular DegU levels and further limit DegU-P formation. However, the present data cannot distinguish between these mechanisms. Further studies are needed to determine how temperature affects DegU phosphorylation, DegU-P stability, and *degU* autoregulation.

Our attempts to stabilize the *swrA* reporter constructs by modifying the homopolymeric A-tract led to the development of the STLich construct, in which the native 8A tract was replaced with a 6A tract mimicking the *B. licheniformis swrA* sequence. Notably, STLich reduced the variability between replicates while displaying fluorescence levels comparable to those of the wild-type *swrA-yfp* construct, making it a promising tool for studying *swrA* expression with a lower impact from spontaneous frameshift mutations. In addition, the development of other stable constructs, in which the poly-A tract was completely removed, revealed an unexpected complexity in the regulation of *swrA* expression. Neither the P_{swrA}-*yfp* construct, in which YFP is placed directly downstream of the *swrA* promoter, nor the Shortissimo construct, in which the first 21 nucleotides of the native *swrA* sequence are fused in frame to YFP, produced detectable YFP fluorescence, despite the detection of Shortissimo mRNA by RT-PCR. This observation suggests that a part of the native *swrA* sequence downstream of the first 21 nucleotides may prevent the formation of an RNA structure that sequesters the RBS and regulates translation. Further studies are required to elucidate whether this proposed RNA-mediated mechanism exists and contributes to the regulation of *swrA* expression.

6.0 References

1) Akinsemolu AA et al. Exploring Bacillus subtilis: ecology, biotechnological applications, and future prospects. J Basic Microbiol. 2024;64:e2300614. doi:10.1002/jobm.202300614.

2) Errington J, van der Aart LT. Microbe Profile: Bacillus subtilis: model organism for cellular development, and industrial workhorse. Microbiology. 2020;166:425-427. doi:10.1099/mic.0.000922.

3) Lopez D et al. Generation of multiple cell types in Bacillus subtilis. FEMS Microbiol Rev. 2009;33:152-163. doi:10.1111/j.1574-6976.2008.00148.x.

4) Earl AM et al. Ecology and genomics of Bacillus subtilis. Trends Microbiol. 2008;16:269-275. doi:10.1016/j.tim.2008.03.004.

5) Blake C et al. Molecular aspects of plant growth promotion and protection by Bacillus subtilis. Mol Plant Microbe Interact. 2021;34:15-25. doi:10.1094/MPMI-08-20-0225-CR.

6) Mohsin MZ et al. Advances in engineered Bacillus subtilis biofilms and spores, and their applications in bioremediation, biocatalysis, and biomaterials. Synth Syst Biotechnol. 2021;6:180-191. doi:10.1016/j.synbio.2021.07.002.

7) Chen YZ et al. Bacillus subtilis: current and future modification strategies as a protein secreting factory. World J Microbiol Biotechnol. 2024;40:195. doi:10.1007/s11274-024-03997-x.

8) Liu ZY, Yu XZ. Engineering Bacillus subtilis for high-value bioproduction: recent advances and applications. Microb Cell Fact. 2025;24:182. doi:10.1186/s12934-025-02818-6.

9) Ishii E, Eguchi Y. Diversity in sensing and signaling of bacterial sensor histidine kinases. Biomolecules. 2021;11:1524. doi:10.3390/biom11101524.

10) Shaw C et al. Two-component systems regulate bacterial virulence in response to the host gastrointestinal environment and metabolic cues. Virulence. 2022;13:1666-1680. doi:10.1080/21505594.2022.2127196.

11) Zschiedrich CP et al. Molecular mechanisms of two-component signal transduction. J Mol Biol. 2016;428:3752-3775. doi:10.1016/j.jmb.2016.08.003.

12) Foulkes DM et al. Regulation of bacterial phosphorelay systems. RSC Chem Biol. 2025;6:1252-1269. doi:10.1039/d5cb00016e.

13) Tzeng YL et al. Phosphorylation of the Spo0B response regulator phosphotransferase of the phosphorelay initiating development in Bacillus subtilis. J Biol Chem. 1998;273:23849-23855. doi:10.1074/jbc.273.37.23849.

14) Fabret C et al. Two-component signal transduction in Bacillus subtilis: how one organism sees its world. J Bacteriol. 1999;181:1975-1983. doi:10.1128/jb.181.7.1975-1983.1999.

15) Hamoen LW et al. Controlling competence in Bacillus subtilis: shared use of regulators. Microbiology. 2003;149:9-17. doi:10.1099/mic.0.26003-0.

16) Dobihal GS et al. Homeostatic control of cell wall hydrolysis by the WalRK two-component signaling pathway in Bacillus subtilis. Elife. 2019;8:e52088. doi:10.7554/eLife.52088.

17) Kobayashi K. Gradual activation of the response regulator DegU controls serial expression of genes for flagellum formation and biofilm formation in Bacillus subtilis. Mol Microbiol. 2007;66:395-409. doi:10.1111/j.1365-2958.2007.05923.x.

18) Yasumura A et al. Involvement of nitrogen regulation in Bacillus subtilis degU expression. J Bacteriol. 2008;190:5162-5171. doi:10.1128/jb.00368-08.

19) Zhou C et al. Regulator DegU can remarkably influence alkaline protease AprE biosynthesis in Bacillus licheniformis 2709. Int J Biol Macromol. 2024;266:130818. doi:10.1016/j.ijbiomac.2024.130818.

20) Murray EJ et al. A pivotal role for the response regulator DegU in controlling multicellular behaviour. Microbiology. 2009;155:1-8. doi:10.1099/mic.0.023903-0.

21) Cairns LS et al. A mechanical signal transmitted by the flagellum controls signalling in Bacillus subtilis. Mol Microbiol. 2013;90(1):6-21. doi:10.1111/mmi.12342.

22) Diethmaier C et al. Viscous drag on the flagellum activates Bacillus subtilis entry into the K-state. Mol Microbiol. 2017;106(3):367-380. doi:10.1111/mmi.13770

23) Henner DJ et al. Localization of Bacillus subtilis sacU(Hy) mutations to two linked genes with similarities to the conserved procaryotic family of two-component signalling systems. J Bacteriol. 1988;170:5102-5109. doi:10.1128/jb.170.11.5102-5109.1988.

24) Mordini S et al. The role of SwrA, DegU and PD3 in fla/che expression in B. subtilis. PLoS One. 2013;8:e85065. doi:10.1371/journal.pone.0085065.

25) Ermoli F et al. SwrA as global modulator of the two-component system DegSU in Bacillus subtilis. Res Microbiol. 2021;172:103877. doi:10.1016/j.resmic.2021.103877.

26) Calvio C et al. Autoregulation of swrAA and motility in Bacillus subtilis. J Bacteriol. 2008;190:5720-5728. doi:10.1128/jb.00455-08.

27) Kearns DB et al. Genes governing swarming in Bacillus subtilis and evidence for a phase variation mechanism controlling surface motility. Mol Microbiol. 2004;52:357-369. doi:10.1111/j.1365-2958.2004.03996.x.

28) Calvio C et al. Swarming differentiation and swimming motility in Bacillus subtilis are controlled by swrA, a newly identified dicistronic operon. J Bacteriol. 2005;187:5356-5366. doi:10.1128/jb.187.15.l5356-5366.2005.

29) Mukherjee S et al. Adaptor-mediated Lon proteolysis restricts Bacillus subtilis hyperflagellation. Proc Natl Acad Sci U S A. 2015;112:250-255. doi:10.1073/pnas.1417419112.

30) Olney SG et al. SmiA is a hybrid priming/scaffolding adaptor for the LonA protease in Bacillus subtilis. J Biol Chem. 2022;298:102045. doi:10.1016/j.jbc.2022.102045.

31) Osera C et al. SwrAA activates poly-γ-glutamate synthesis in addition to swarming in Bacillus subtilis. Microbiology. 2009;155:2282-2287. doi:10.1099/mic.0.026435-0.

32) Popović M et al. Disruption of bacteriophage integration site promotes rapid diversification of multicellular traits in Bacillus subtilis. Microbiol Spectr. 2026;14:e02504-25. doi:10.1128/spectrum.02504-25.

33) Kearns DB, Losick R. Cell population heterogeneity during growth of Bacillus subtilis. Genes Dev. 2005;19:3083-3094. doi:10.1101/gad.1373905.

34) van Gestel J et al. Bacillus subtilis in defense mode: switch-like adaptations to protistan predation. Proc Natl Acad Sci U S A. 2025;122:e2518989122. doi:10.1073/pnas.2518989122.

35) Ogunleye A et al. Poly-γ-glutamic acid: production, properties and applications. Microbiology. 2015;161:1-17. doi:10.1099/mic.0.081448-0

36) Nair P et al. Poly-gamma-glutamic acid biopolymer: a sleeping giant with diverse applications and unique opportunities for commercialization. Biomass Convers Biorefin. 2023;13:4555-4573. doi:10.1007/s13399-021-01467-0.

37) Ogasawara Y et al. Involvement of Peptide Epimerization in Poly-γ-glutamic Acid Biosynthesis. Org Lett. 2019;21:3972-3975. doi:10.1021/acs.orglett.9b01121.

38) Hsueh YH et al. Poly-γ-glutamic acid synthesis, gene regulation, phylogenetic relationships, and role in fermentation. Int J Mol Sci. 2017;18:2644. doi:10.3390/ijms18122644.

39) Scoffone V et al. Knockout of *pgdS* and *ggt* genes improves γ-PGA yield in *B. subtilis*. Biotechnol Bioeng. 2013;110:2006-2012. doi:10.1002/bit.24846.

40) Stanley NR, Lazazzera BA. Defining the genetic differences between wild and domestic strains of Bacillus subtilis that affect poly-γ-DL-glutamic acid production and biofilm formation. Mol Microbiol. 2005;57:1143-1158. doi:10.1111/j.1365-2958.2005.04746.x.

41) Deol R et al. Poly-Gamma-Glutamic Acid Secretion Protects Bacillus subtilis from Zinc and Copper Intoxication. Microbiol Spectr. 2022;10:e01329-21. doi:10.1128/spectrum.01329-21.

42) Jang J et al. The poly-γ-D-glutamic acid capsule of Bacillus anthracis enhances lethal toxin activity. Infect Immun. 2011;79:3846-3854. doi:10.1128/IAI.01145-10.

43) Kocianova S et al. Key role of poly-γ-DL-glutamic acid in immune evasion and virulence of Staphylococcus epidermidis. J Clin Invest. 2005;115:688-694. doi:10.1172/JCI23523.

44) Yu Y et al. Poly-γ-glutamic acids contribute to biofilm formation and plant root colonization in selected environmental isolates of Bacillus subtilis. Front Microbiol. 2016;7:1811. doi:10.3389/fmicb.2016.01811.

45) Chou TKT et al. Self-generated hydrogel ejects bacterial cells for localized biofilm dispersion. Nat Microbiol. 2026. doi:10.1038/s41564-026-02413-4.

46) Morris RJ et al. Density and temperature controlled fluid extraction in a bacterial biofilm is determined by poly-γ-glutamic acid production. NPJ Biofilms Microbiomes. 2022;8:98. doi:10.1038/s41522-022-00361-5.

47) Narberhaus F et al. RNA thermometers. FEMS Microbiol Rev. 2006;30:3-16. doi:10.1111/j.1574-6976.2005.004.x.

48) Kortmann J, Narberhaus F. Bacterial RNA thermometers: molecular zippers and switches. Nat Rev Microbiol. 2012;10:255-265. doi:10.1038/nrmicro2730.

49) Loh E et al. RNA thermometers in bacterial pathogens. Microbiol Spectr. 2018;6:RWR-0012-2017. doi:10.1128/microbiolspec.rwr-0012-2017.

50) Jolley EA et al. Transcriptome-wide probing reveals RNA thermometers that regulate translation of glycerol permease genes in Bacillus subtilis. RNA. 2023;29:1365-1378. doi:10.1261/rna.079652.123.

51) Nguyen QA et al. Construction of plasmid-based expression vectors for *Bacillus subtilis* exhibiting full structural stability. Plasmid. 2005;54:241-248. doi:10.1016/j.plasmid.2005.04.001.

52) Veening JW et al. Visualization of differential gene expression by improved cyan fluorescent protein and yellow fluorescent protein production in *Bacillus subtilis*. Appl Environ Microbiol. 2004;70(11):6809-6815. doi:10.1128/AEM.70.11.6809-6815.2004.

53) Ogura M, Tsukahara K. Autoregulation of the Bacillus subtilis response regulator gene degU is coupled with the proteolysis of DegU-P by ClpCP. Mol Microbiol. 2010;75:1244-1259. doi:10.1111/j.1365-2958.2010.07047.x.